PECS Project No. 98056

GOCE – specific tasks on fine gravity field structure of the Earth

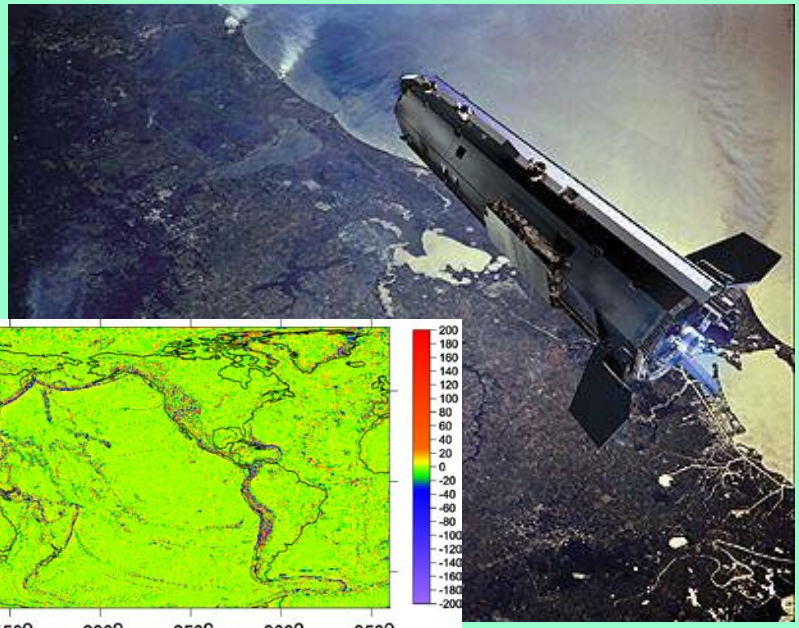

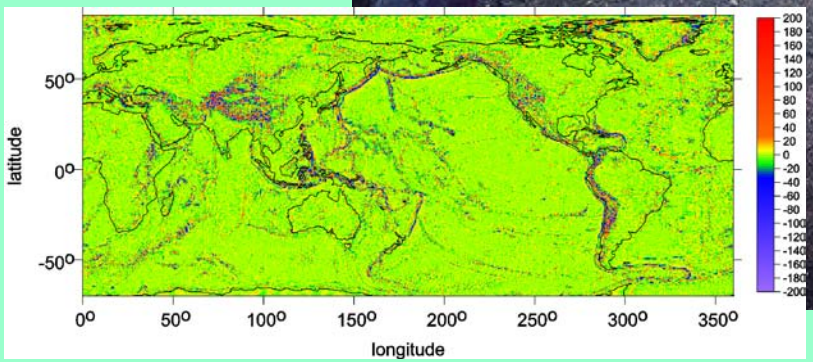

PI: Jaroslav Kloko• ník,
Astronomical Institute of the ASCR,v.v.i., Ond•ejov Observatory

Prepared by
A. Bezd• k, J. Kloko• ník, J. Kostelecký, P. Novák, J. Sebera, I. Pešek

Presented by
J. Kloko• ník

Project team

- Jaroslav Kloko• ník (PI), Astronomical Institute of the ASCR

- Aleš Bezd• k, Astronomical Institute of the ASCR

- Josef Sebera, Astronomical Institute of the ASCR

- Jan Kostelecký, Faculty of Civil Engineering, CTU Prague

- Ivan Pešek, Faculty of Civil Engineering, CTU Prague

- Pavel Novák, Department of Mathematics, University of West Bohemia, Pilsen

Project activities during 2010

1. **Orbit choice and tuning for GOCE measuring phases**
   (responsible person: Aleš Bezd• k)

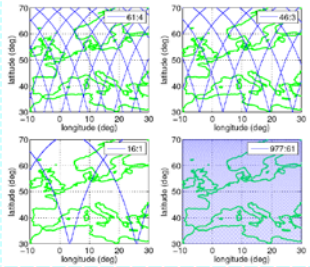

2. **Novel geodetic computational methodologies**
   (responsible person: Josef Sebera)

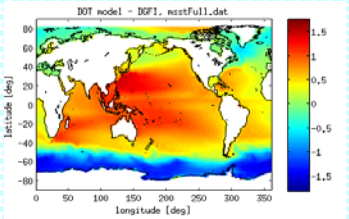

3. **Comparison of detailed satellite and terrestrial data**
   (responsible person: Pavel Novák)

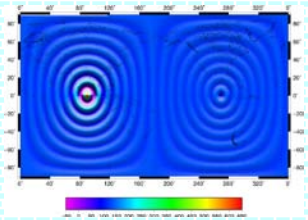

4. **Detection of hidden impact (meteoritic) structures on the Earth surface**
   (responsible person: Jaroslav Kloko• ník)

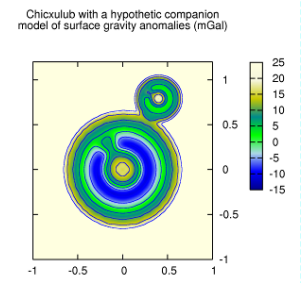

Publications in 2010

- Published papers: 11
- Submitted manuscripts: 3
- Presentations and posters: 9

Duration of PECS project: 1 Sep 2007 – 1 Sep 2011

(we are asking to prolong it untill the end of 2011)

Orbit choice and tuning for GOCE measuring phases & the inversion for the gravity field parameters

(responsible person: A. Bezd• k)

- Fine orbit tuning for GOCE as a result of previous analyses of CHAMP and GRACE resonances
- Generalized view for planetary orbiters
- Generalized least-squares adjustment for the gravity field parameters, our first attempts

Orbital resonances

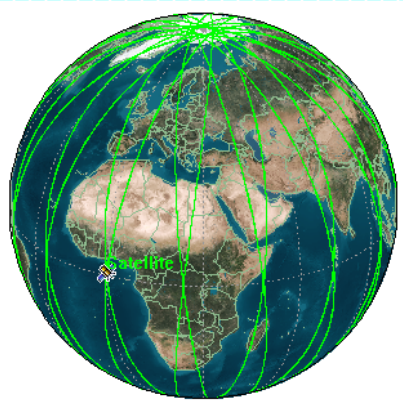

Orbital resonance **R:D** takes place, if:

- Groundtracks are exactly the same after **R** nodal revolutions and **D** nodal days
- Equivalent names: repeat orbit, exact repeat mission

- Modelling of gravity field
  - Dense enough grid of groundtracks
  - Rule of thumb (from Nyquist theorem): $\mathbf{n_{max} < R/2}$

  n_{max} maximum degree/order

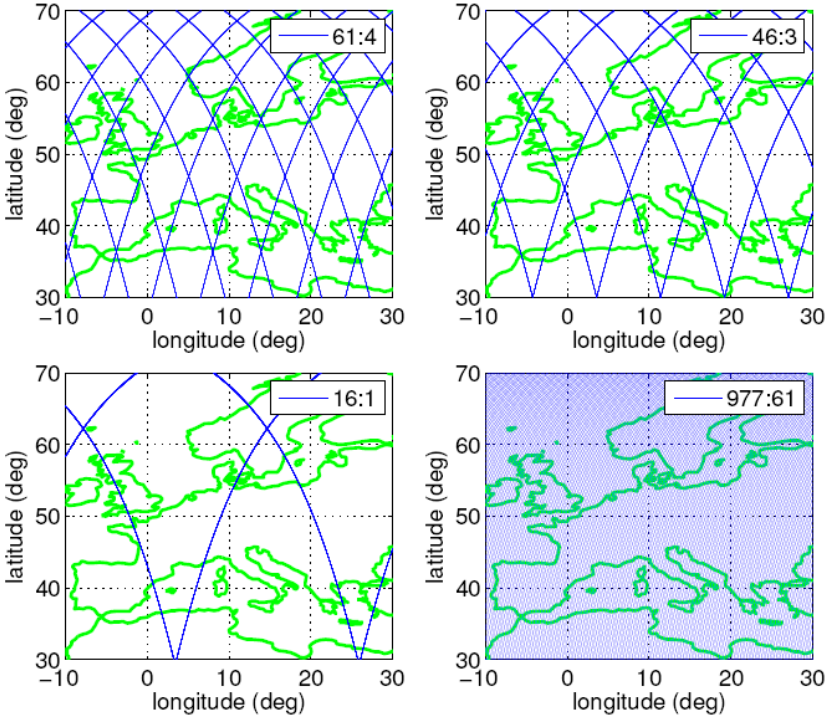

Orbital resonances and quality of gravity field models

- CHAMP: 46/3, 31/2, 47/3, 16/1 (decayed in Sep 2010)
- GRACE: 61/4
  - Worse quality of monthly gravity solutions in Aug/Sep 2004
- GOCE: 16/1
  - Avoiding gradiometer measurements near the 16/1 repeat orbit

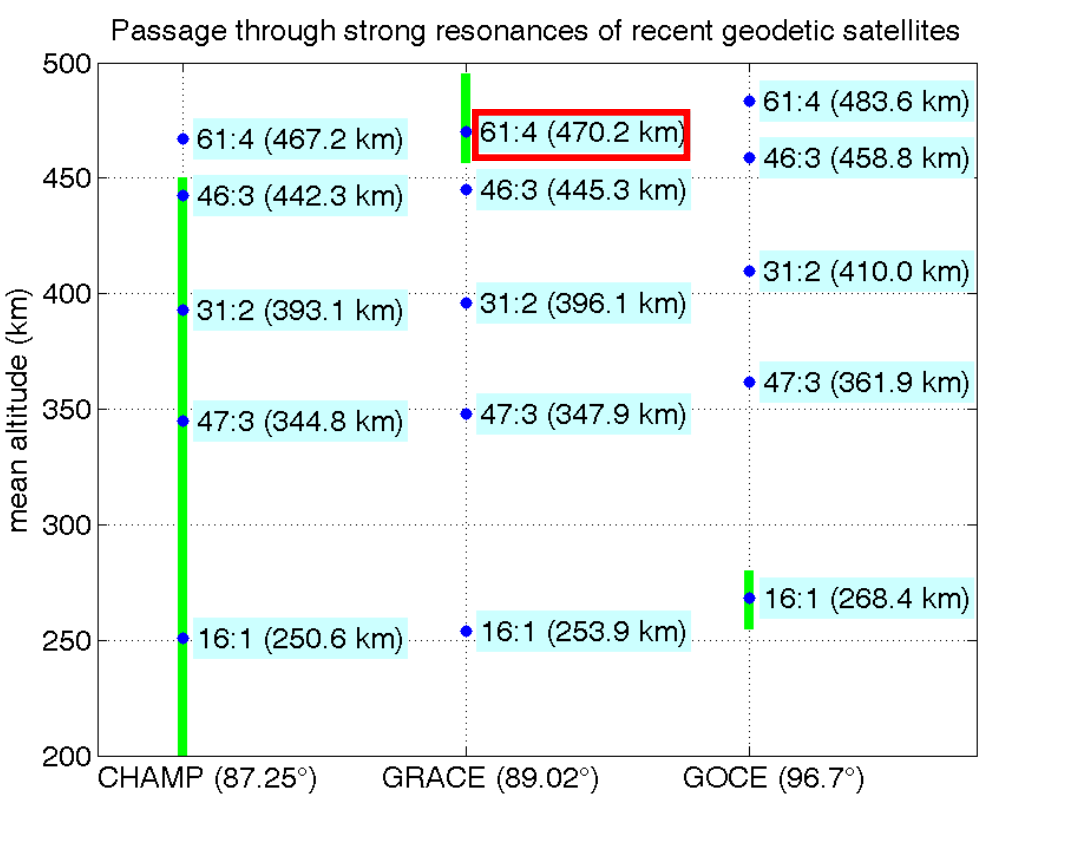

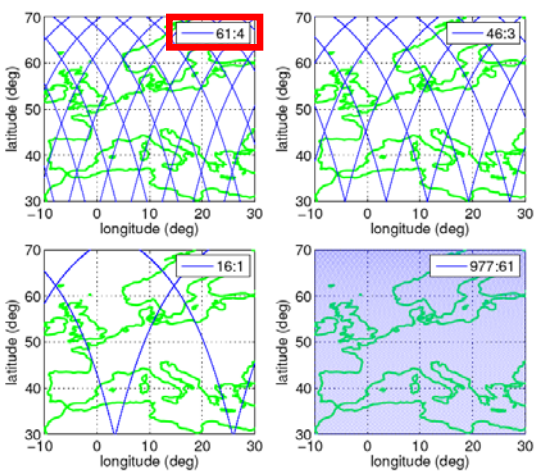

Example – passage of GRACE through 61:4 resonance

- August–September 2004
  - larger degree error in gravity monthlies

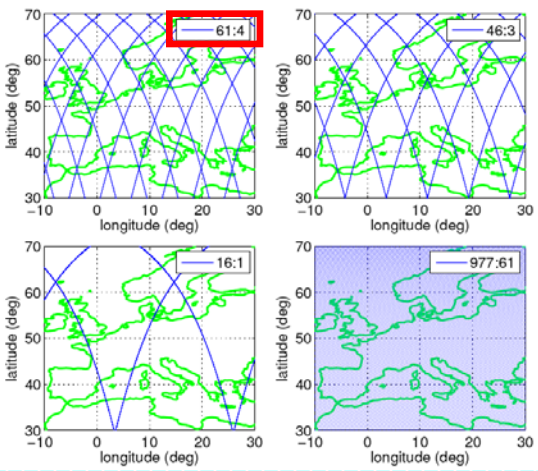

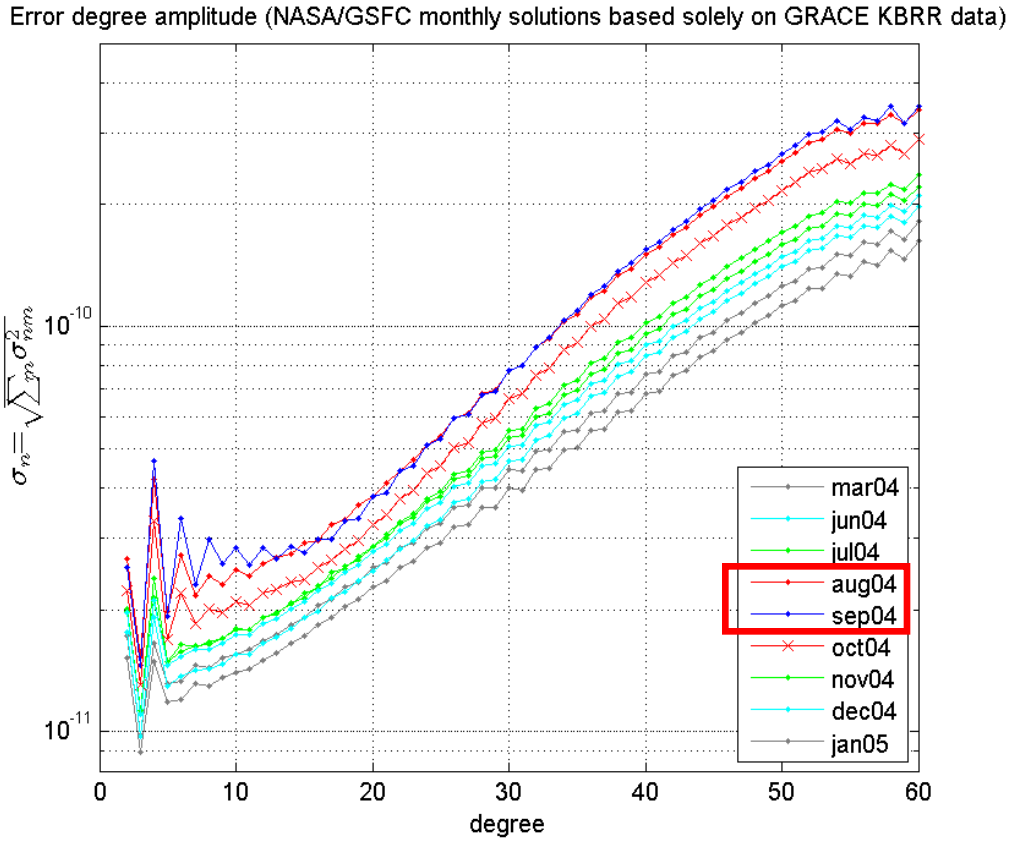

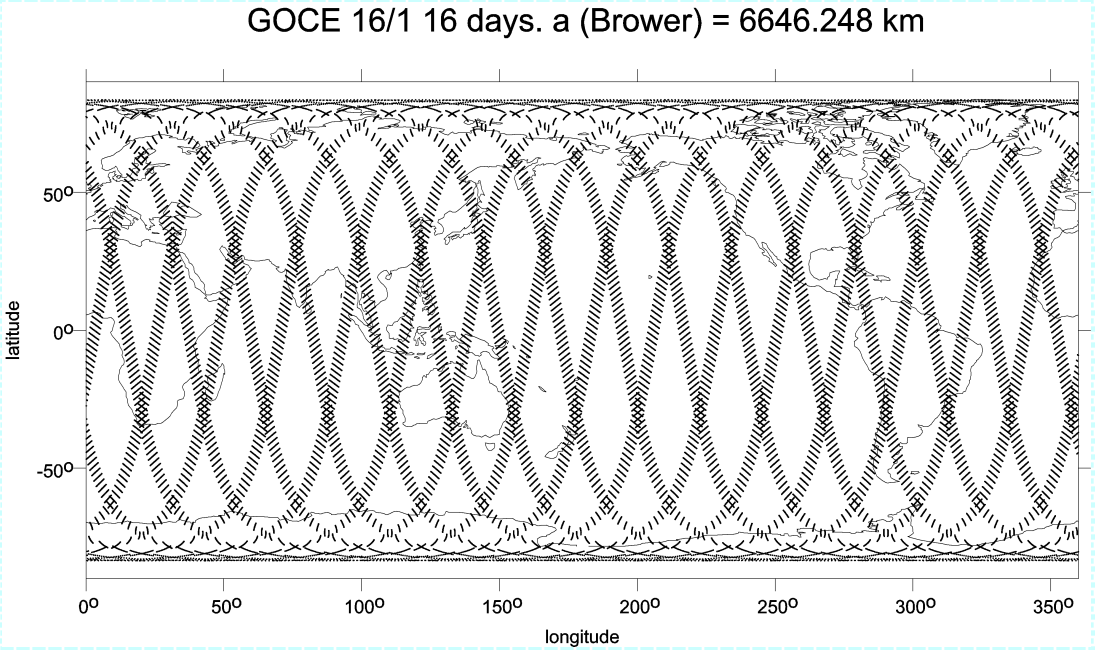
GOCE 16/1 16 days. a (Brower) = 6646.248 km
50°
0°
-50°
latitude
0°
50°
100°
150°
200°
250°
300°
350°
longitude

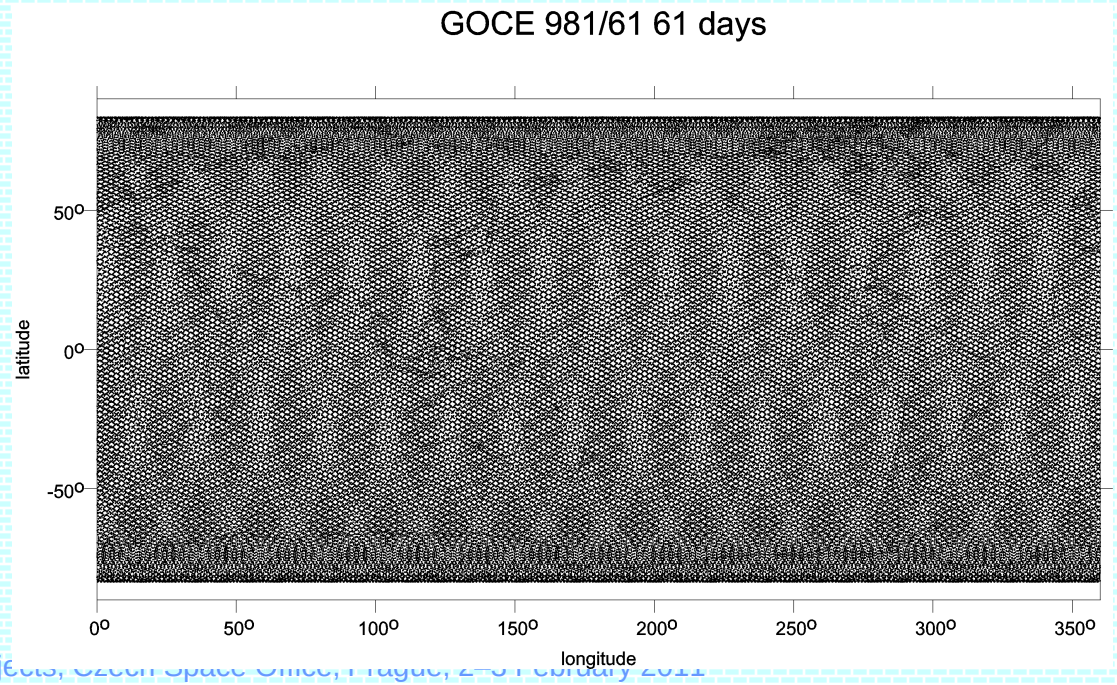
GOCE 981/61 61 days
50°
0°
-50°
latitude
0°
50°
100°
150°
200°
250°
300°
350°
longitude

GOCE – scientific objectives

- To determine the **geoid** with a radial accuracy of 1–2 cm
- To achieve this **globally** at length scales down to 100 km
  - maximum degree/order ~250
  - minimum repeat period of **2 months**

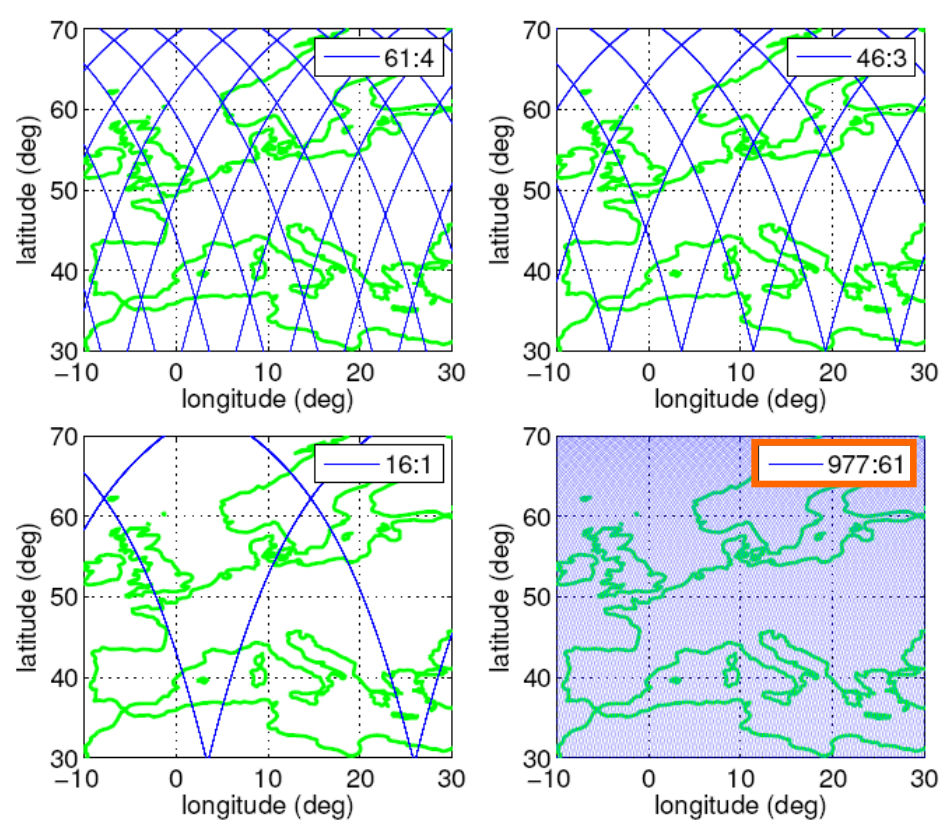

Gradiometer – main payload of GOCE

- Six accelerometers
  - ➢ mounted in pairs along three perpendicular axes
  - ➢ 0.5 m arm length

- Measured quantity: differences in gravity acceleration
  - tensor of gravity gradients

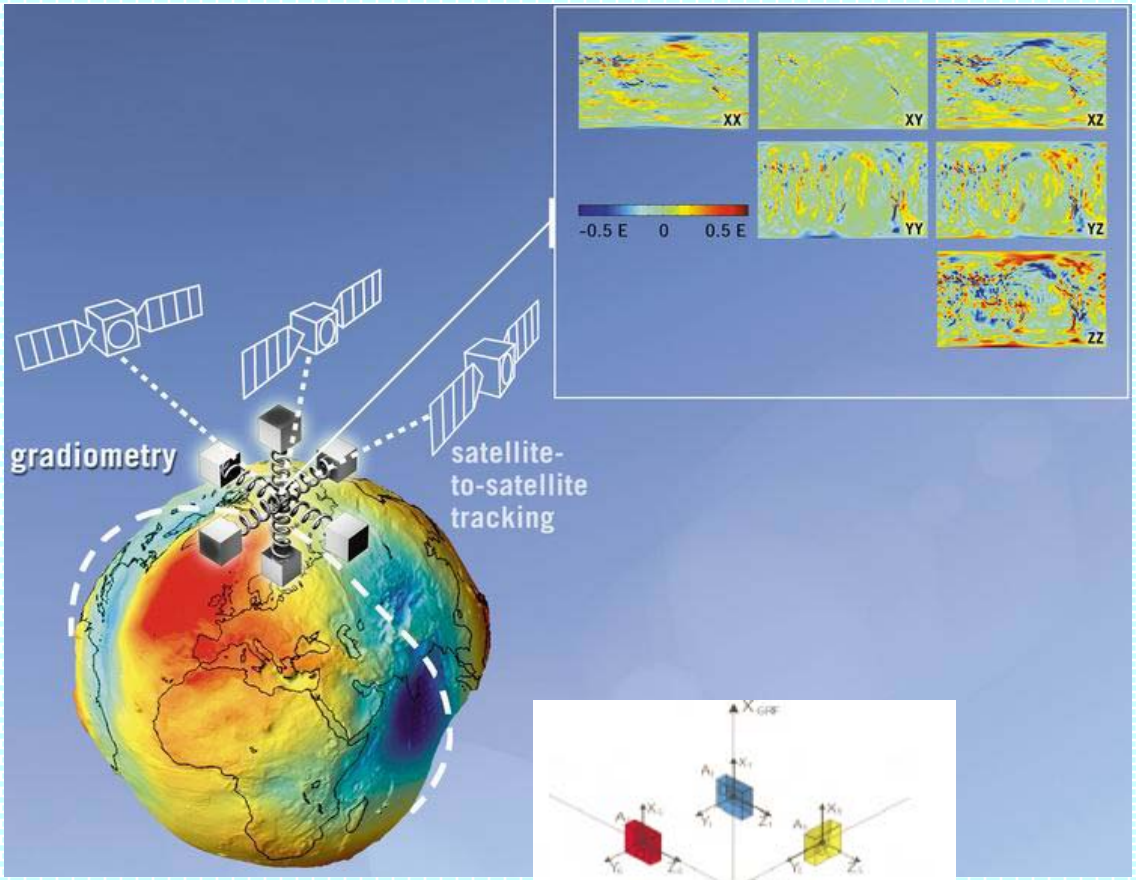

Temporal evolution of an orbit – with/without a subcycle

- Repeat orbit
  with **no subcycles**
  - gradually filling up
  two large equatorial gaps

- Repeat orbit
  with a **subcycle**
  - groundtracks laid down in two (or more) almost homogeneous grids

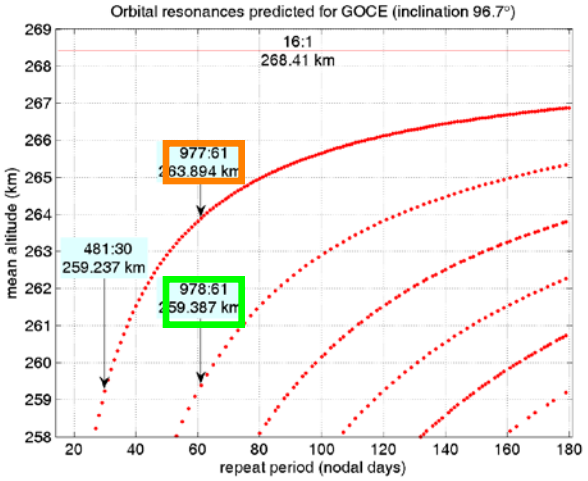

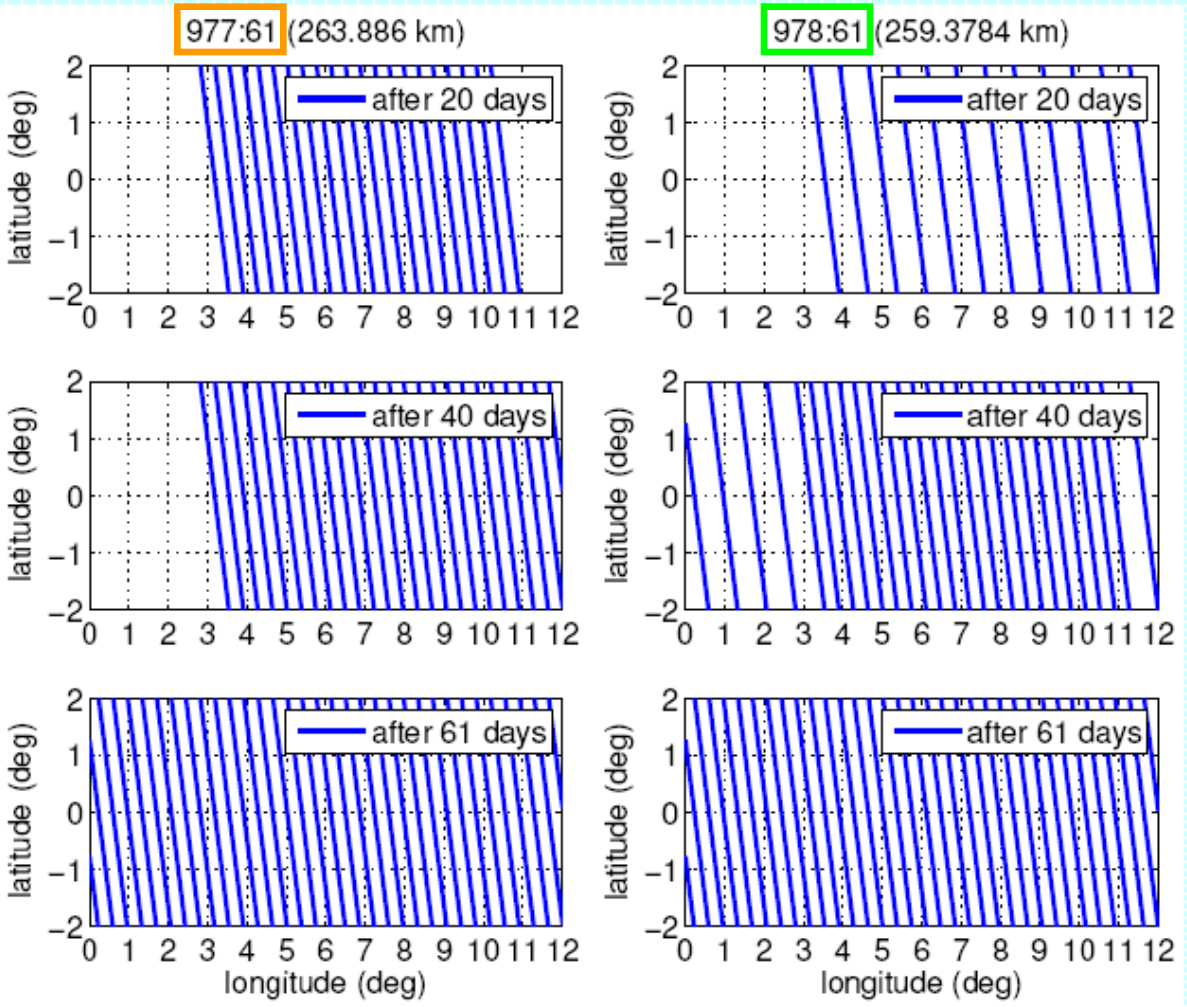

The 145-day orbit with 62/83 day subcycles

Suggested repeat orbit for 2011 **2327:145**
node spacing • **17.2 km**

Nearest repeat orbits

- **62**-day, lower by **30 m**
- **83**-day, higher by **23 m**

Ion thruster performance ±10 m

145-day repeat is a good choice

- node spacing at least
  - **40.3 km** for **62**-day repeat
  - **30.1 km** for **83**-day repeat

Resonant orbits ordered by height		
D	R	h (km)
1653	103	255,062
995	**62**	255,105
2327	**145**	255,135
1332	**83**	255,158
1669	104	255,19
2006	125	255,211
2343	146	255,226

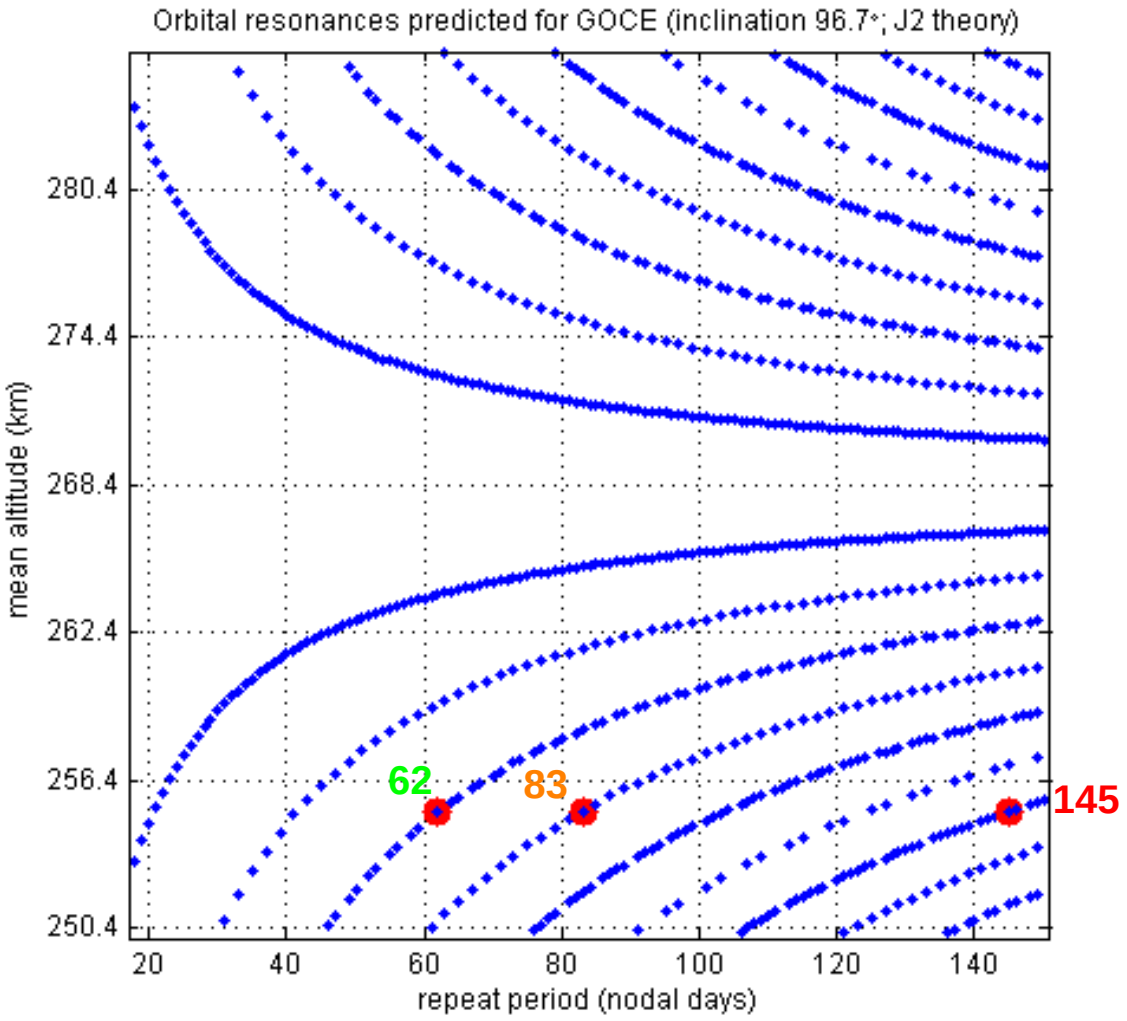

Gravity field from kinematic positions

- Kinematic positions **r** • by using **second-derivative digital filter F**
  - GPS-based (observed) accelerations $d^2\mathbf{r}/dt^2$ • $\mathbf{a}_{GPS}$ • $F * r$

- **Newton second law**:

$$\mathbf{a}_{GPS} \bullet\ d^2\mathbf{r}/dt^2 = \mathbf{a}_{geop} + \mathbf{a}_{LS} + \mathbf{a}_{TID} + \mathbf{a}_{NG} \qquad (1)$$

  where the accelerations are due to

  $\mathbf{a}_{geop}(\mathbf{r})$ • $\sum$ SP×SSH(r,• ,•) … geopotential in spherical harmonics SSH
  SP…Stokes parameters

  $\mathbf{a}_{LS}$ … lunisolar effects
  $\mathbf{a}_{TID}$ … solid Earth and ocean tides
  $\mathbf{a}_{NG}$ … acc. of nongravitational origin (drag, radiation pressures)

- From (1) a **linear system** is set up:

$$\sum \text{SP}\times\text{SSH}(r,\bullet,\bullet) = \mathbf{a}_{GPS} - (\mathbf{a}_{LS} + \mathbf{a}_{TID} + \mathbf{a}_{NG}) \qquad (2)$$

- **Stokes parameters (SP)** may be obtained directly from eq. (2)

- To solve the system in Eq. (2) we make use of the **Generalized least squares** (**GLS**)

GLS inversion of gravity parameters: GOCE (1 day; max. degree 15)

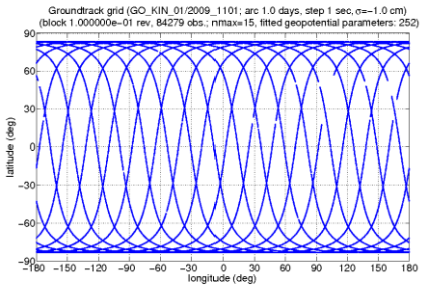

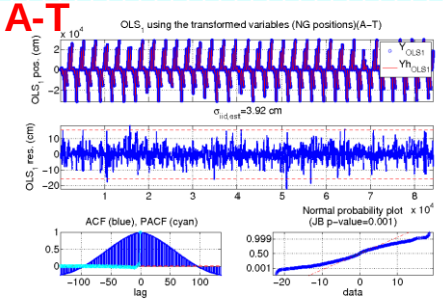

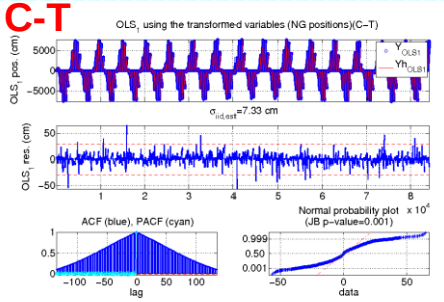

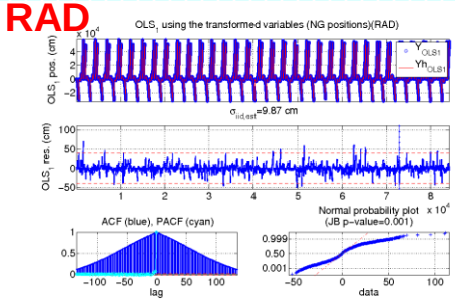

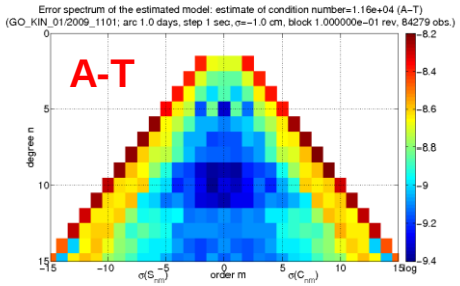

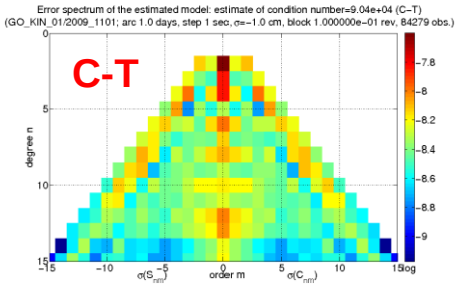

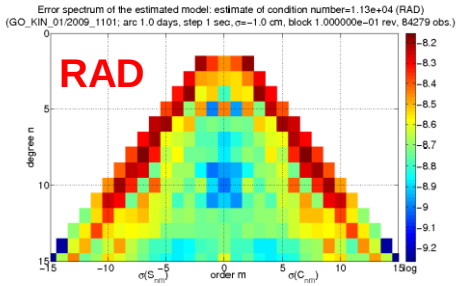

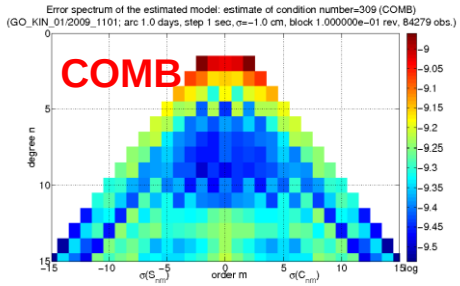

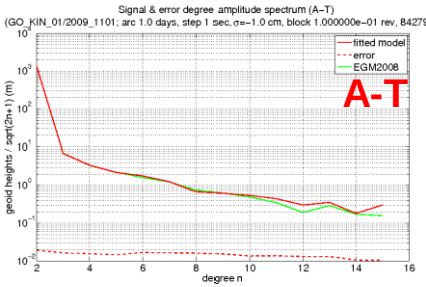

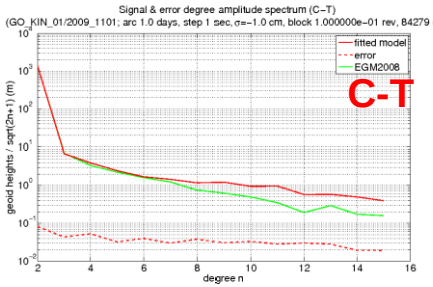

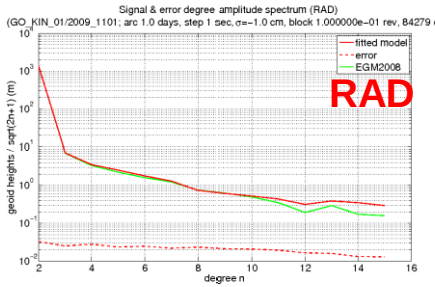

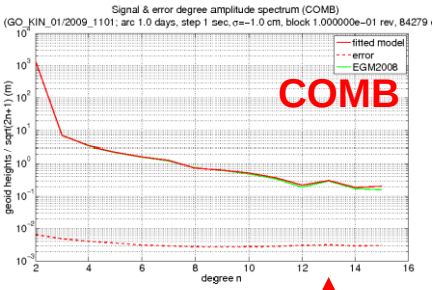

- Better results in higher degrees due to finer sampling (1 sec vs. 10 sec. of GRACE A)

Geoid heights of the combined GLS solution for GRACE, GOCE vs. EGM08

- Solutions up to degree/order 15 were obtained from 1 day of GPS orbital data
- Figures show that gravity field parameters from orbits of both satellites give reasonable results

GRACE A

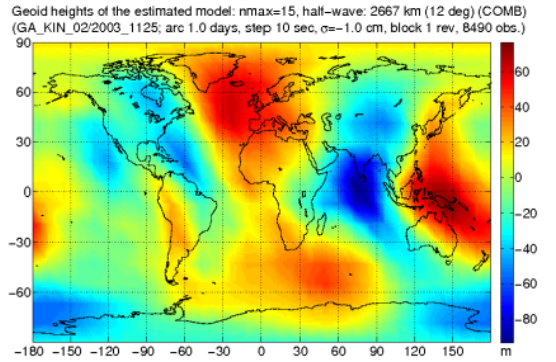

GOCE

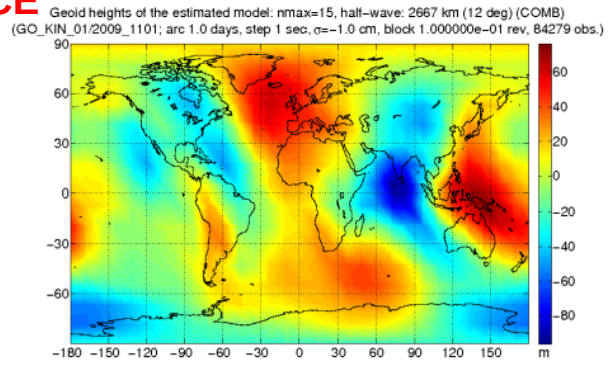

EGM 2008

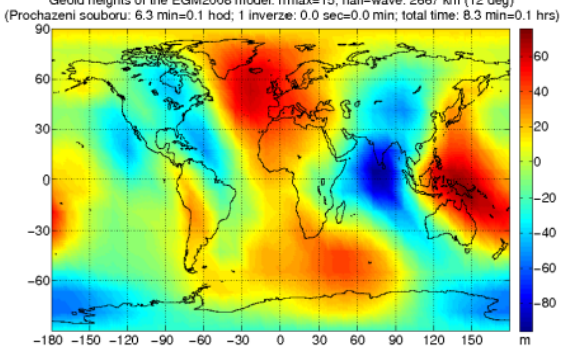

PLANETS

$\dot{S}$

Basic dynamic parameters of the Earth and other bodies of the solar system				
body	**GM [km^{3}s^{-2}]**	**J_2 [10^{-6}]**	**R [m]**	**[rev/day]**
Earth	398600.44	1082.627	6378137	1.00274
Moon	4902.80	203.428	1738140	0.03660
Mercury	22032.24	60	2439700	0.01705
Venus	324858.36	5.97	6051800	-0.00411
Mars	42828.37	1959.2	3396190	0.97470

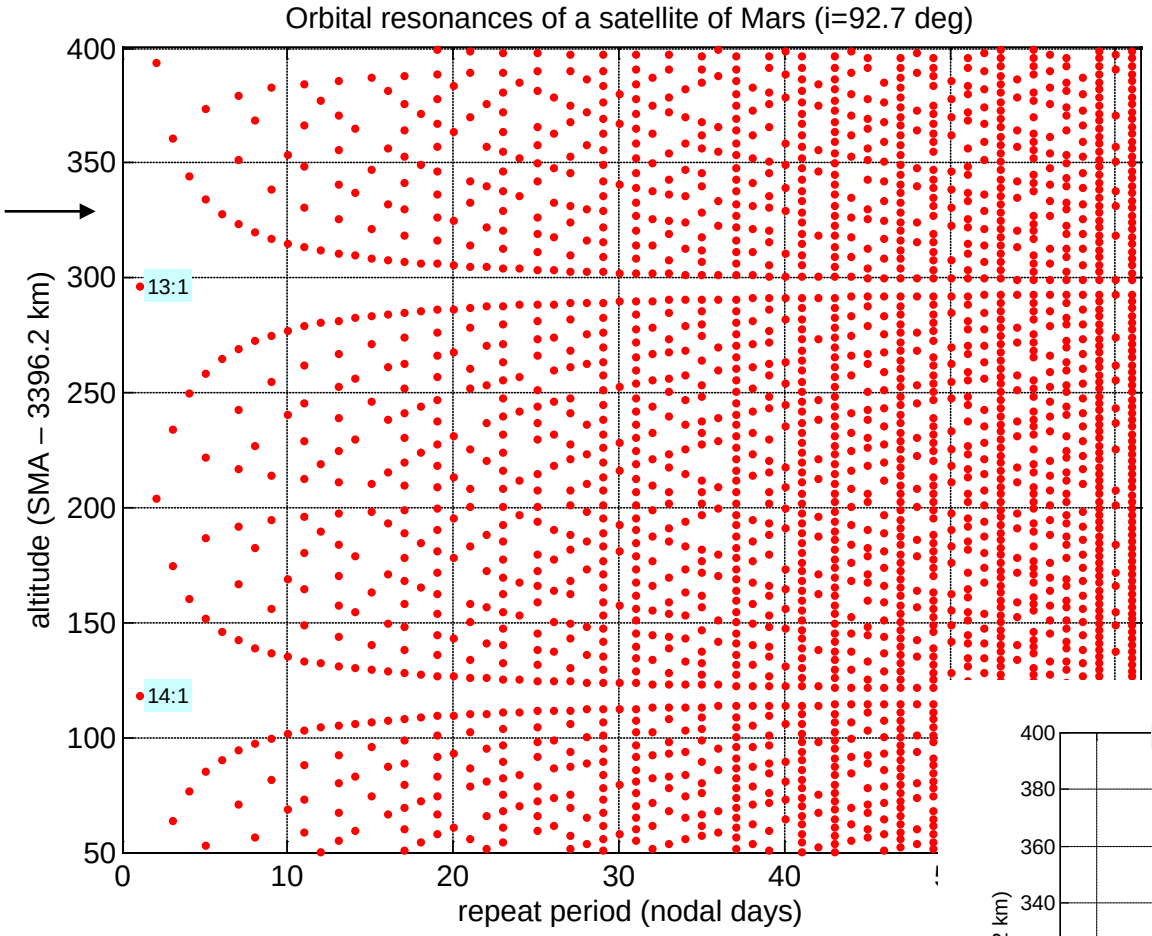
Orbital resonances of a satellite of Mars (i=92.7 deg)
altitude (SMA – 3396.2 km)
repeat period (nodal days)
13:1
14:1
400
350
300
250
200
150
100
50
0
10
20
30
40

MARS

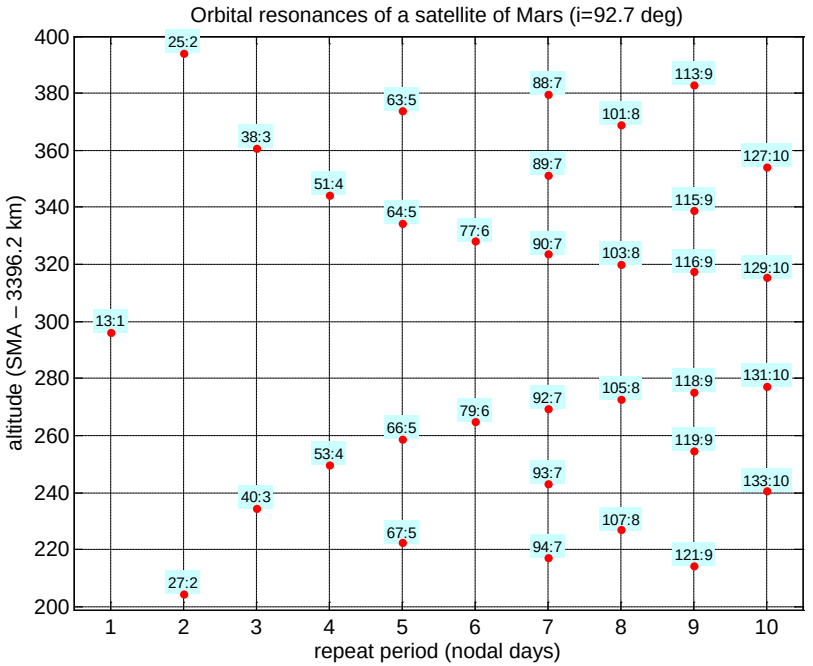
Orbital resonances of a satellite of Mars (i=92.7 deg)
altitude (SMA – 3396.2 km)
repeat period (nodal days)
25:2
38:3
51:4
63:5
64:5
66:5
53:4
40:3
67:5
27:2
13:1
77:6
79:6
88:7
89:7
90:7
92:7
93:7
94:7
101:8
103:8
105:8
107:8
113:9
115:9
116:9
118:9
119:9
121:9
127:10
129:10
131:10
133:10
400
380
360
340
320
300
280
260
240
220
200
1
2
3
4
5
6
7
8
9
10

Lmax < R/2!

MARS

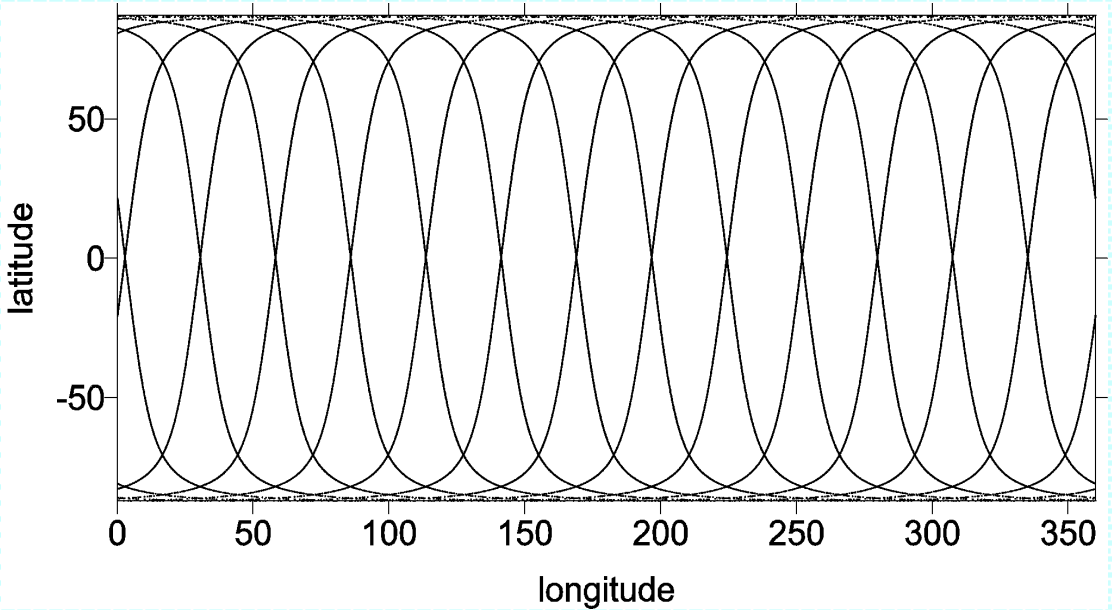

Ground tracks for a Mars orbiter at the 13:1 and 188:15

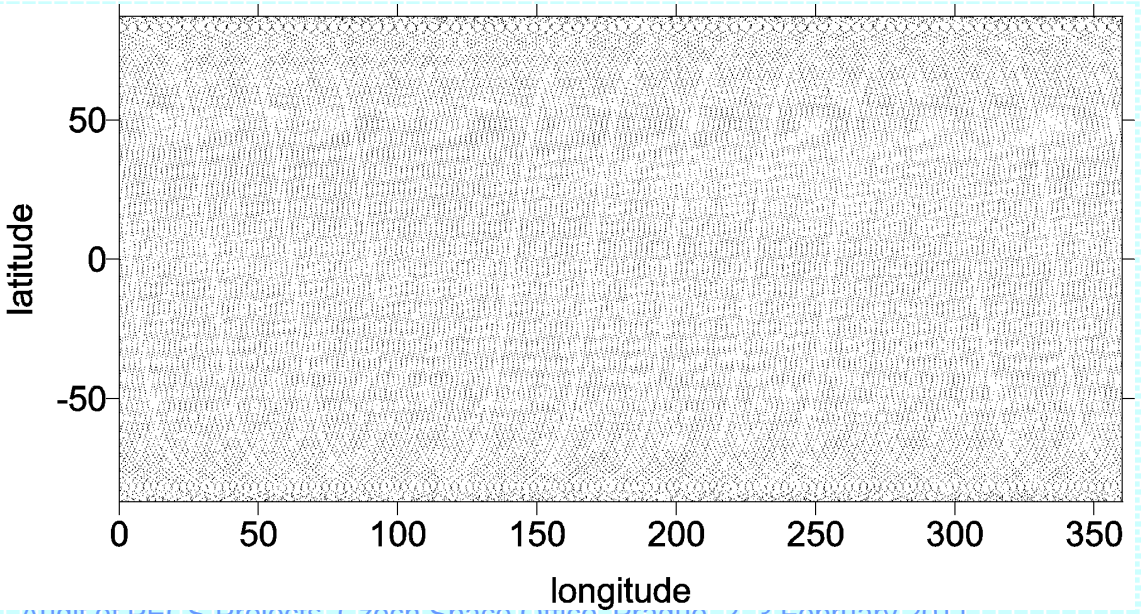

density *D* at 13:1 is 1640 km, *D* at 188:15 is ~~ 110 km

The MOON

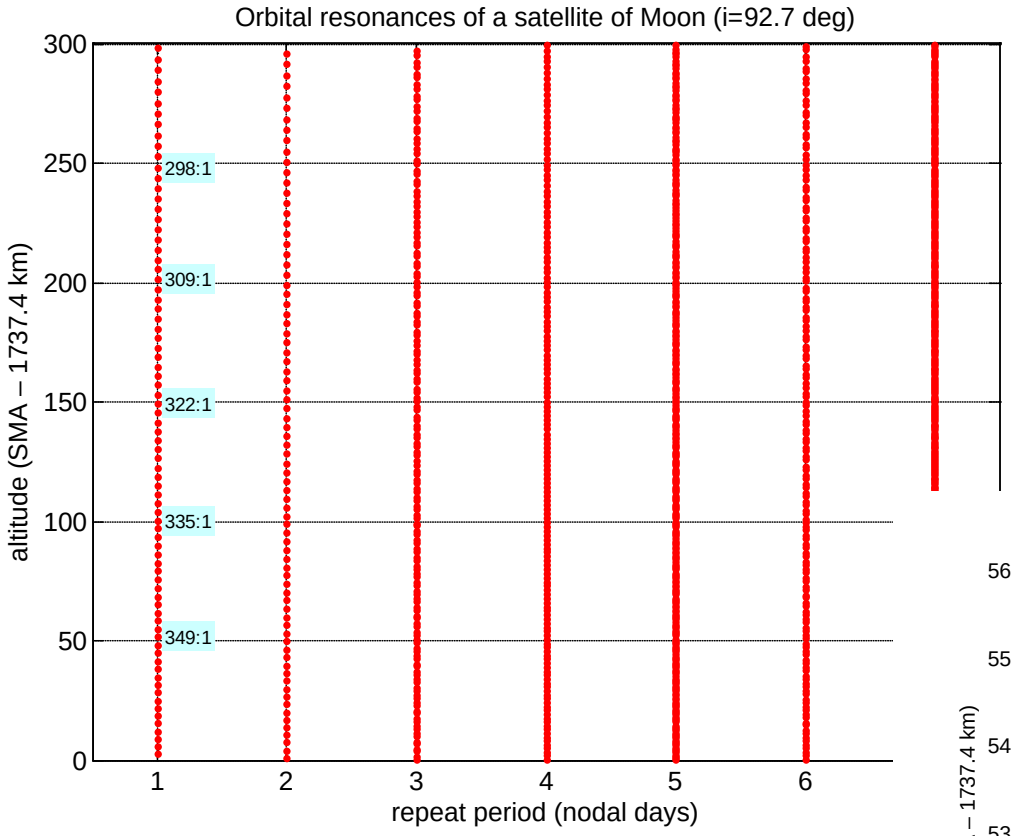
Orbital resonances of a satellite of Moon (i=92.7 deg)
altitude (SMA – 1737.4 km)
repeat period (nodal days)
298:1
309:1
322:1
335:1
349:1

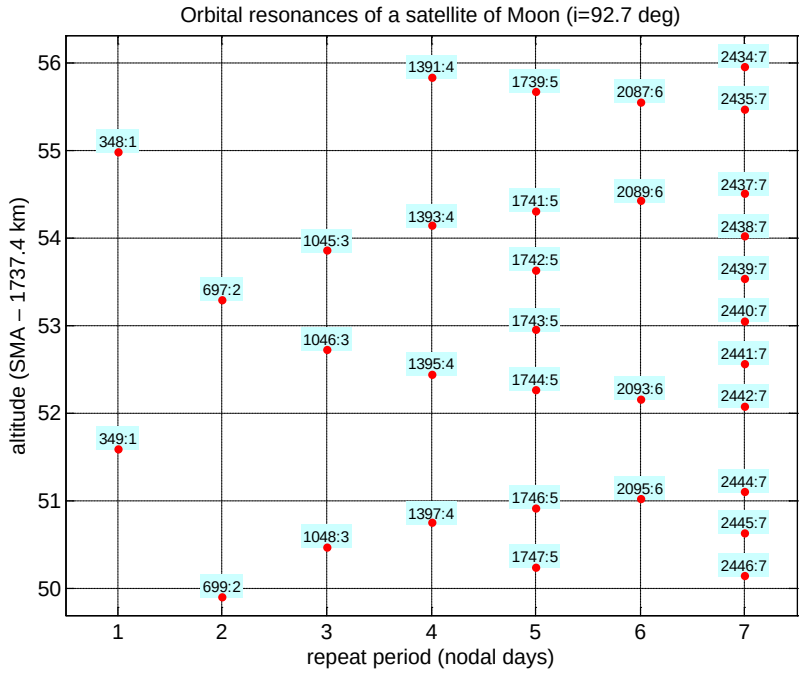
Orbital resonances of a satellite of Moon (i=92.7 deg)
altitude (SMA – 1737.4 km)
repeat period (nodal days)
348:1
349:1
697:2
699:2
1045:3
1046:3
1048:3
1391:4
1393:4
1395:4
1397:4
1739:5
1741:5
1742:5
1743:5
1744:5
1746:5
1747:5
2087:6
2089:6
2093:6
2095:6
2434:7
2435:7
2437:7
2438:7
2439:7
2440:7
2441:7
2442:7
2444:7
2445:7
2446:7

MERCURY

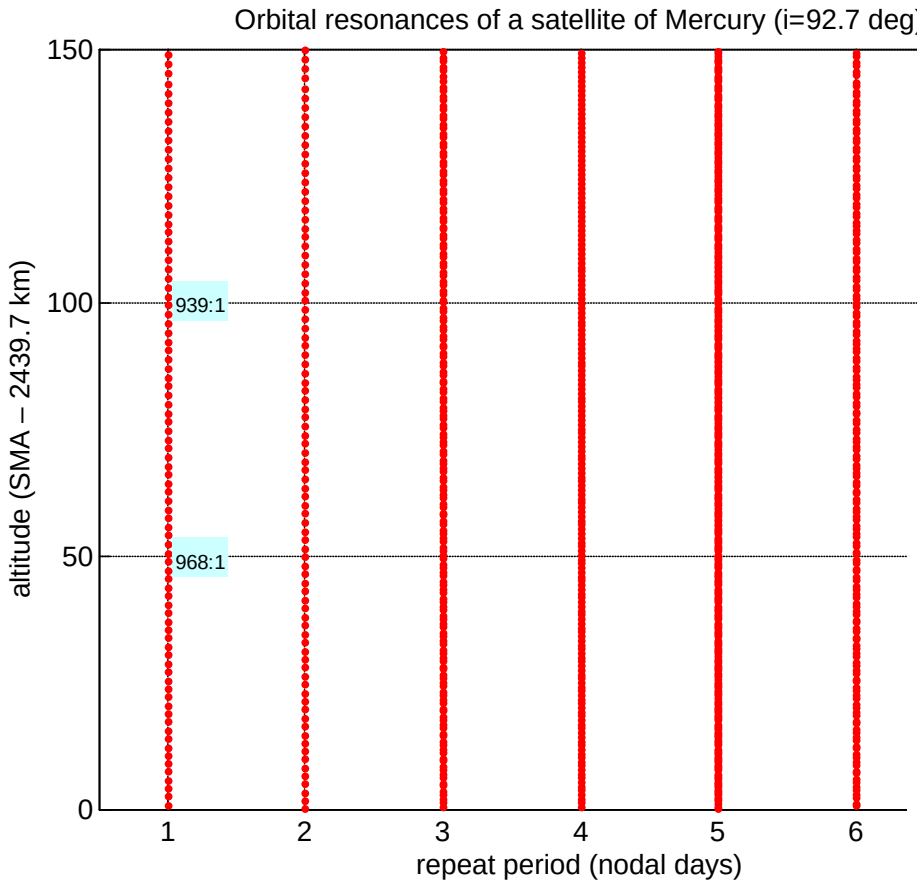
Orbital resonances of a satellite of Mercury (i=92.7 deg)
altitude (SMA – 2439.7 km)
repeat period (nodal days)
939:1
968:1

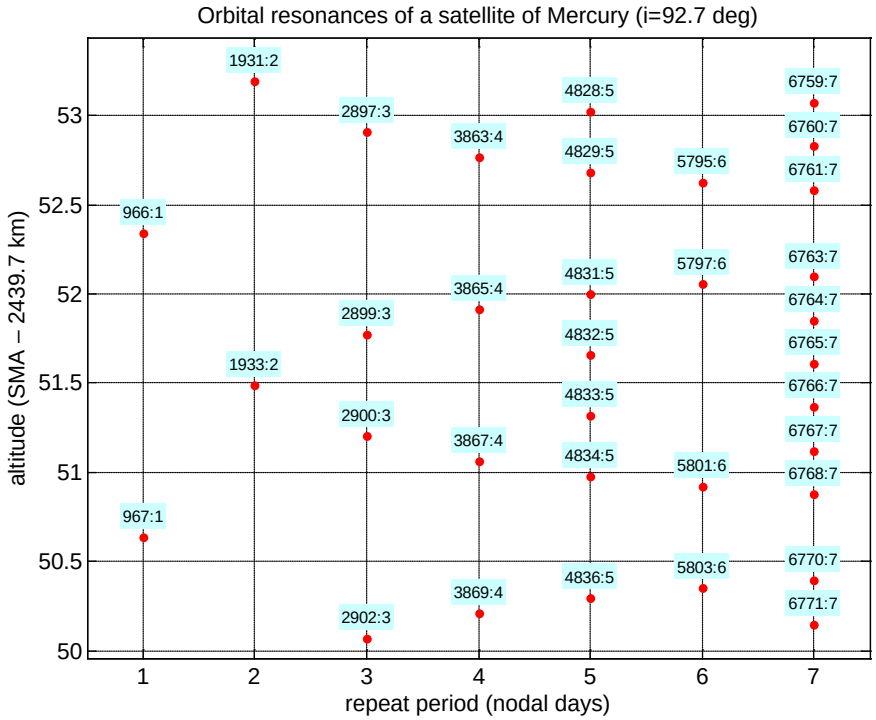
Orbital resonances of a satellite of Mercury (i=92.7 deg)
altitude (SMA – 2439.7 km)
repeat period (nodal days)
966:1
967:1
1931:2
1933:2
2897:3
2899:3
2900:3
2902:3
3863:4
3865:4
3867:4
3869:4
4828:5
4829:5
4831:5
4832:5
4833:5
4834:5
4836:5
5795:6
5797:6
5801:6
5803:6
6759:7
6760:7
6761:7
6763:7
6764:7
6765:7
6766:7
6767:7
6768:7
6770:7
6771:7

VENUS

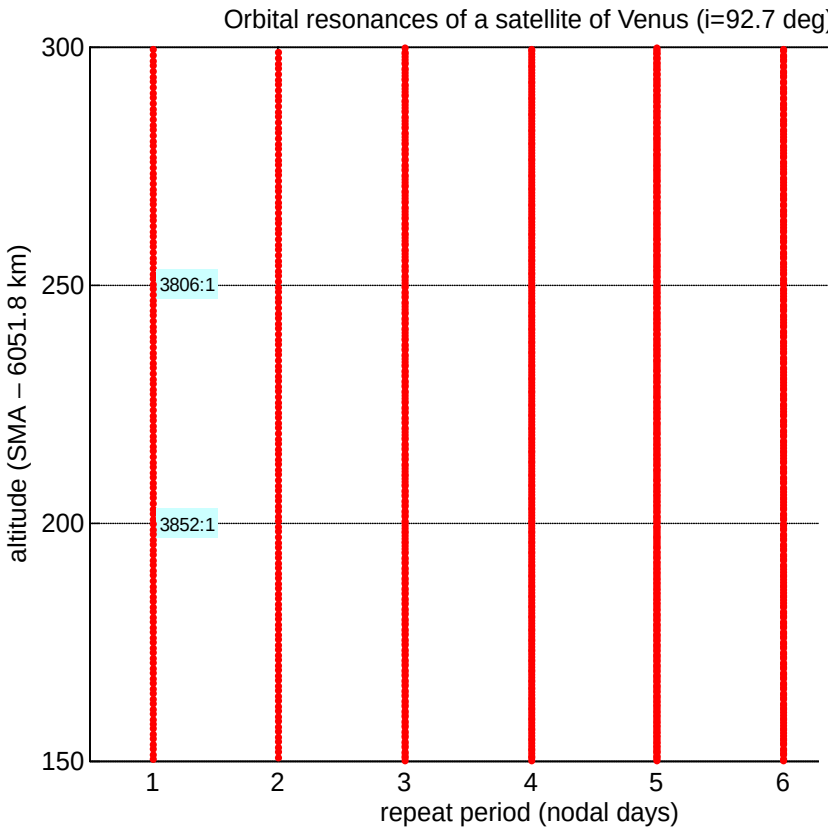
Orbital resonances of a satellite of Venus (i=92.7 deg)
altitude (SMA – 6051.8 km)
repeat period (nodal days)
300
250
200
150
1
2
3
4
5
6
3806:1
3852:1

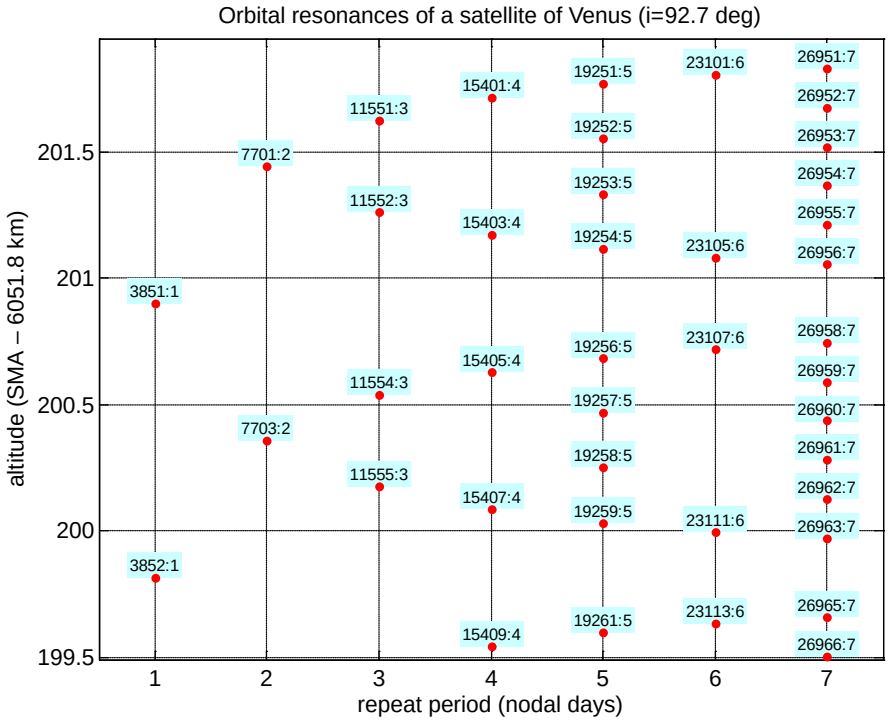
Orbital resonances of a satellite of Venus (i=92.7 deg)
altitude (SMA – 6051.8 km)
repeat period (nodal days)
201.5
201
200.5
200
199.5
1
2
3
4
5
6
7
3851:1
3852:1
7701:2
7703:2
11551:3
11552:3
11554:3
11555:3
15401:4
15403:4
15405:4
15407:4
15409:4
19251:5
19252:5
19253:5
19254:5
19256:5
19257:5
19258:5
19259:5
19261:5
23101:6
23105:6
23107:6
23111:6
23113:6
26951:7
26952:7
26953:7
26954:7
26955:7
26956:7
26958:7
26959:7
26960:7
26961:7
26962:7
26963:7
26965:7
26966:7

Rationale behind fine orbit tuning & conclusions

- Without “good” coverage even the most sophisticated space instrument would not produce “good” geopotential coefficients!
- CHAMP and GRACE experience • ESA sought for optimally dense and regular groundtracks grid
- Direct relationship between the density of satellite ground tracks and accuracy of the gravity field parameters derived, inherent presence of orbit resonances, intentional orbit tuning as a tool to maximize accuracy gain in the gravity field mapping
- Special situation of GOCE

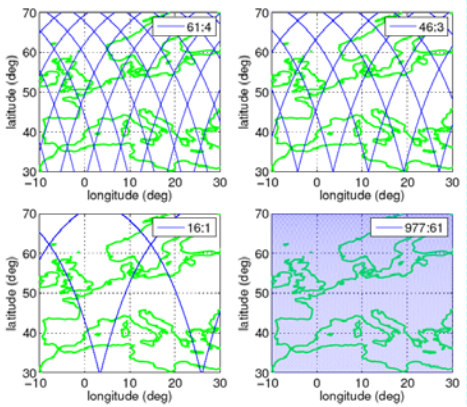

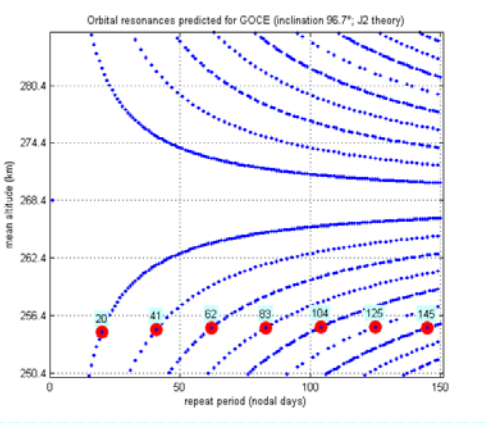

- A small shift in altitude may considerably affect the full utilization of the accuracy of the instrument
- Heights of highlighted orbits: only ±180 m, groundtrack density is extremely different
- Highlighted orbits also differ in regularity of their coverage pattern
- For planetary orbiters,a problem for Mars (not for slowly rotating Venus, Mercury or the Moon, ***Lmax < < R.***)

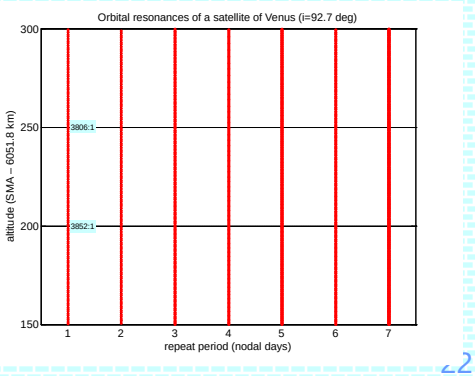

- ***Published or presented contributions:***

1. Bezd• k A, Kloko• ník J, Kostelecký J, Floberghagen R, Sebera J, 2010. Some aspects of the orbit selection for the measurement phases of GOCE. Proceedings of the ESA Living Planet Symposium, Bergen, Norway, 28 June–2 July, ESA SP-686.
2. Bezd• k A, Kloko• ník J, Kostelecký J, Floberghagen R, Sebera J, 2010. Fine orbit tuning to increase the accuracy of the gravity-field modelling. Presented at 2010 AGU Fall Meeting, 13–17 December, Moscone Convention Center, San Francisco, California, USA.
3. Kloko• ník J, Bezd• k A, Kostelecký J, Sebera J, 2010. Orbit tuning of planetary orbiters for accuracy gain in gravity-field mapping. Journal of guidance, control, and dynamics 33(3), 853–861. http://dx.doi.org/10.2514/1.46223
4. Kloko• ník J., Bezd• k A., Kostelecký J., Orbit tuning for GOCE measuring phases and for planetary orbiters to maximize accuracy gain in the gravity field mapping, pres. at session 4 „Earth Obs. Systems…“, WEGENER 2010, 15th Gen. Assembly Wegener, Sept. 14-17, 20010, Istanbul, Turkey.
5. Kloko• ník J, Bezd• k A, Kostelecký J. GNSS-R concept extended by a fine orbit tuning, ESA Workshop on GNSS-R 2010, Barcelona (poster, now paper in review)

Novel geodetic computational methodologies
(responsible person: J. Sebera)

a) Satellite altimetry and gradiometry

- With DGFI we use the mean curvature of the sea surface to derive the second radial derivative of the gravitational potential Vzz. Why? ...this quantity is to be used to calibrate measurements on GOCE satellite.
- Dynamic Ocean Topography(DOT) as a water surplus causes disturbances in derived signal: dVzz
- There are more models of DOT, so we have in addition an error from modelling.

Signal: dVzz (globally) [1e9/s^2]

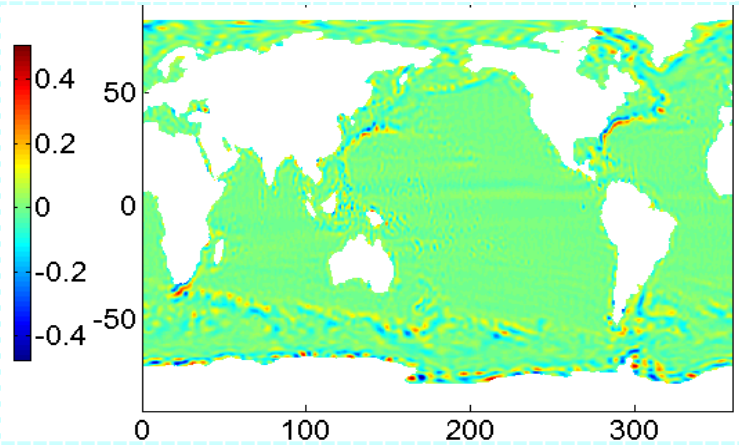

←COMPARE→
Error is 1/10 of the signal!

Error of dVzz from DOT 5 models [1e9/s^2]

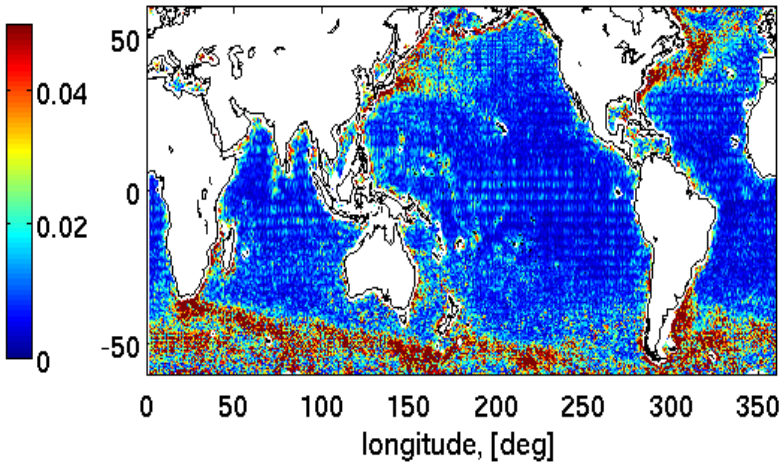

Histogram of this error [%]

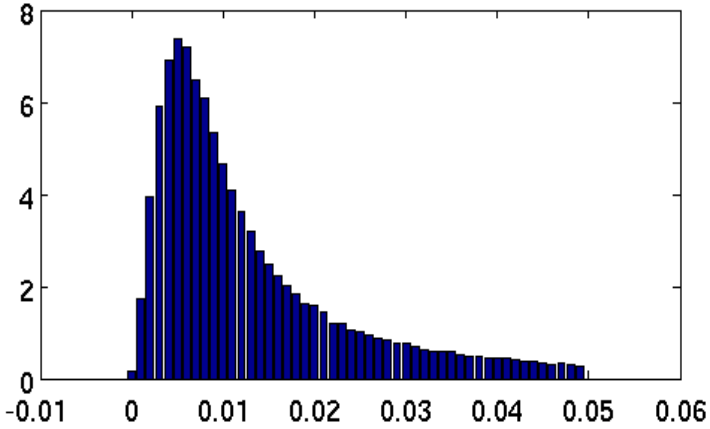

Conclusions:

- Curvature approach successfully implemented and tested for grid computations – must be generalized
- In areas of ocean currents we can expect larger errors of DOT models
- Thus: better to use satellite altimetry data out of these areas.
- In next step the data must be upward continued
- **See Sebera: DGFI report**

b) Straightforward parametrization of the Eötvös tensor (Direct approach)

- Parametrization ~ observation equation = way from measurements to unknowns (geopotential parameters in spherical harmonic series).
- We have used Hotine's formalism to define rotated observations equations.
- Why? ...GOCE gives Vxx,Vyy,Vzz,Vxz,Vxy,Vyz, but in general frame as the satellite shakes while orbiting due to orbit perturbations. The blue measurements are of high accuracy, the red ones of less accuracy due to gradiometer construction.
- If the tensor would be rotated into conventional frame and then processed, the red ones would “contaminate“ the whole tensor (see note below)!
- Thus, we have decided to not rotate data themselves but rotate the observation equations.

The key is to work with tensor rotation analytically, so putting eqs. on right into equation below yields the rotated observation equations

$$V'_{ij} = R_{(I,II,...n)} T_{ij} R^T_{(I,II,...n)} = S \cdot V_{ij},$$

$$\begin{pmatrix} V'_{xx} \\ V'_{yy} \\ V'_{zz} \\ V'_{xy} \\ V'_{xz} \\ V'_{yz} \end{pmatrix} = \begin{pmatrix} s_{11} & s_{12} & s_{13} & s_{14} & s_{15} & s_{16} \\ s_{21} & s_{22} & s_{23} & s_{24} & s_{25} & s_{26} \\ s_{31} & s_{32} & s_{33} & s_{34} & s_{35} & s_{36} \\ s_{41} & s_{42} & s_{43} & s_{44} & s_{45} & s_{46} \\ s_{51} & s_{52} & s_{53} & s_{54} & s_{55} & s_{56} \\ s_{61} & s_{62} & s_{63} & s_{64} & s_{65} & s_{66} \end{pmatrix} \cdot \begin{pmatrix} V_{yz} \\ V_{yy} \\ V_{zz} \\ V_{xy} \\ V_{xz} \\ V_{yz} \end{pmatrix}$$

Note that each component on left is a linear combination of all components on right

Hotine's formalism provides all tensor components in the same form

$$\begin{aligned}
V_{xx} &= K \sum_{n,m} A_n \left(C^{xx}_{n+2,m} \cos m\lambda + S^{xx}_{n+2,m} \sin m\lambda \right) \bar{P}_{n+2,m}(\cos\theta) \\
V_{yy} &= K \sum_{n,m} A_n \left(C^{yy}_{n+2,m} \cos m\lambda + S^{yy}_{n+2,m} \sin m\lambda \right) \bar{P}_{n+2,m}(\cos\theta) \\
V_{zz} &= K \sum_{n,m} A_n \left(C^{zz}_{n+2,m} \cos m\lambda + S^{zz}_{n+2,m} \sin m\lambda \right) \bar{P}_{n+2,m}(\cos\theta) \\
V_{xy} &= K \sum_{n,m} A_n \left(C^{xy}_{n+2,m} \cos m\lambda + S^{xy}_{n+2,m} \sin m\lambda \right) \bar{P}_{n+2,m}(\cos\theta) \\
V_{xz} &= K \sum_{n,m} A_n \left(C^{xz}_{n+2,m} \cos m\lambda + S^{xz}_{n+2,m} \sin m\lambda \right) \bar{P}_{n+2,m}(\cos\theta) \\
V_{yz} &= K \sum A_n \left(C^{yz}_{n+2,m} \cos m\lambda + S^{yz}_{n+2,m} \sin m\lambda \right) \bar{P}_{n+2,m}(\cos\theta)
\end{aligned}$$

Conclusions:

- Concept derived and successfully implemented in Matlab
- Now we want to move in more efficient software tools as the problem is really huge ... several millions of data and 65 000 uknowns!
- Strong numerical libraries and parallelization needed
- **See Sebera: Poster at EGU 2010, Vienna**

c) Computing ellipsoidal harmonics and their “tuning”

- When modelling the Earth's gravitational field globally, the standard(traditional) tool is to work with spherical harmonics. However, the Earth is more an ellipsoid than a sphere. To decrease the approximation error we started with the ellipsoidal approximation in terms of ellipsoidal harmonics.

Spherical harmonics **vs.** **Ellipsoidal harmonics with Jekeli's renormalization**

$$V(r,\theta,\lambda) = \frac{GM}{R}\sum_{n=0}^{\infty}\sum_{m=0}^{n}\left(\frac{R}{r}\right)^{n+1}\left(\bar{C}^{s}_{n,m}\cos m\lambda + \bar{S}^{s}_{n,m}\sin m\lambda\right)\bar{P}_{n,m}(\cos\theta)$$

$$V(u,\vartheta,\lambda) = \frac{GM}{R}\sum_{n=0}^{\infty}\sum_{m=0}^{n}\frac{\bar{S}_{n,m}\left(\frac{u}{E}\right)}{\bar{S}_{n,m}\left(\frac{b}{E}\right)}\left(\bar{C}^{e}_{n,m}\cos m\lambda + \bar{S}^{e}_{n,m}\sin m\lambda\right)\bar{P}_{n,m}(\cos\vartheta)$$

$|\nabla T|$

Successfull tests: e.g. for $|\partial T|$ about 12 valid digits!

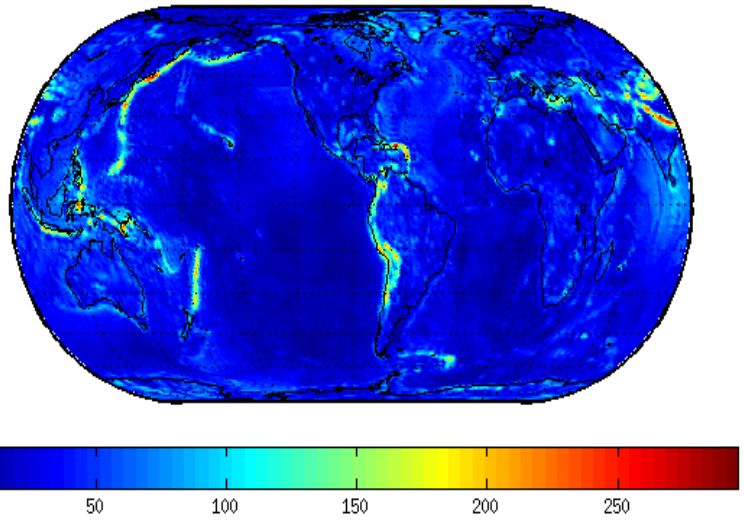

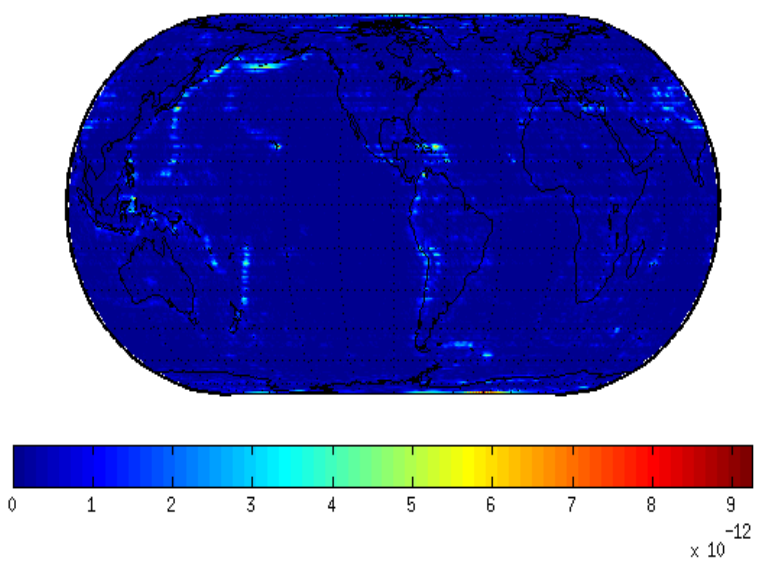

Conclusions:

- We prepared new algorithms for Legedre functions of the 2nd kind and its two derivatives within the hypergeometric formulation with help of Jekeli's renormalization
- High accuracy for all derivatives to degree/order 2190 achieved
- **See Sebera: Submitted paper to Journal of Geodesy**

- ***Published or submitted contributions:***

1. Sebera J., Bouman J., Bosch W., Dynamic ocean topography and vertical gravity gradient computation, DGFI Report 87, November 2010.
2. Sebera J., Wagner C.A., Bouman J., Bezd• k A., Kloko• ník J., Kostelecký J., Novák P., Gravitational tensor in the GOCE reference frame by direct harmonic synthesis. Pres. at EGU GA Vienna 2010, Geophys. Res. Abstracts 12, EGU2010-7103-3, 2010.
3. Sebera J., Bosch W., Bouman J., Kostelecký J., Kloko• ník J., Bezd• k A. Upward continuation of satellite altimeter data for GOCE validation. Pres. at the ESA Living Planet Symposium, Bergen, Norway, 28 June – 2 July 2010.
4. Sebera J., Bouman J., Bosch W., On computing ellipsoidal harmonics using Jekeli's renormalization, Journal of Geodesy (submitted).

Comparison of detailed satellite and terrestrial data
(responsible person: P. Novák)

Data combination

- Earth's gravitational field described by the potential *V*
- spaceborne data of type GOCE represent in-situ *grad* ⊗ *grad V*
- ground (airborne, marine) data correspond to *grad V*
- all data used for derivation of the potential *V*
- for the general data type *f(V)* the inversion can be done through

$$f(V) = \frac{1}{S} \iint_{s} V(S)\, f(K)\, dS$$

with the functional of the Abel-Poisson kernel function *f(V)*

Combination through integral inversion

- for GOCE $f = grad \otimes grad$, for ground gravity $f = e \cdot grad$
  (for a unit vector e along a local plumbline - local vertical)
- tensor-values integration kernel for GOCE : $grad \otimes grad\, K$

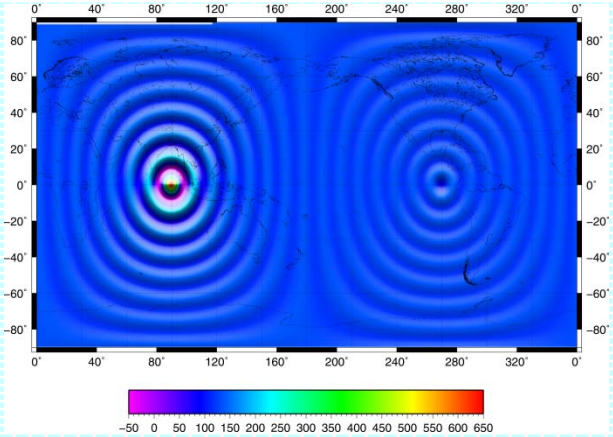

$h^2_r\, D^2_r$

$h_r\, h_\phi\, D^2_{r\phi}$

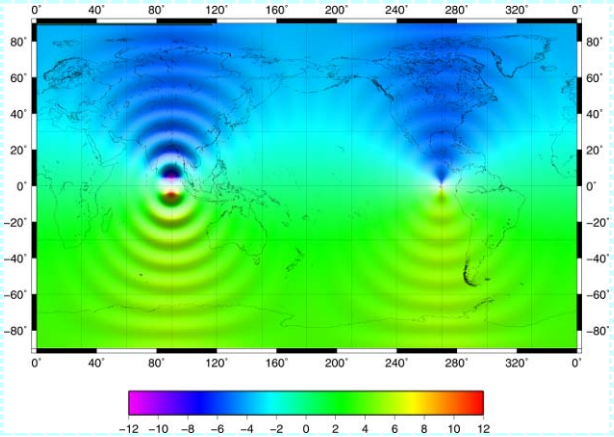

$h_r\, h_\lambda\, D^2_{r\lambda}$

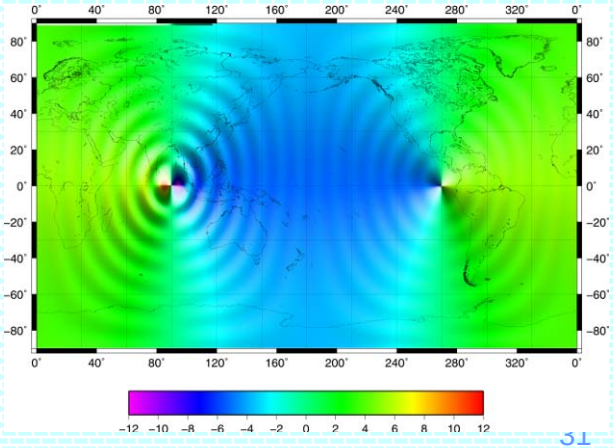

- ***Published or submitted contributions:***

1. Novák P (2010). High resolution constituents of the Earth gravitational field. *Surveys in Geophysics* 31(1): 1-21, doi: 10.1007/s10712-009-9077-z.
2. Novák P (2010). Direct modeling of the gravitational field using harmonic series. *Acta Geodynamica at Geomaterialia* 157(1): 35-47.
3. Kloko• ník J, Kostelecký J, Novák P, Wagner CA (2010). Detection of Earth impact craters aided by the detailed global gravitational model EGM2008. *Acta Geodynamica at Geomaterialia* 157(1): 71-97.
4. Vajda P, Ellmann A, Meurers B, Vaní• ek P, Novák P, Tenzer R (2010). Harmonic continuation and gravimetric inversion of gravity in areas of negative geodetic heights. In Mertikas SP (ed.) *Gravity, Geoid and Earth Observation*: 25-30, Springer-Verlag Berlin Heidelberg, ISBN: 978-3-642-10633-0.
5. Vajda P, Vaní• ek P, Novák P, Tenzer R, Ellmann A, Meurers B (2010). On ambiguities in definitions and applications of Bouguer gravity anomaly. In Mertikas SP (ed.) *Gravity, Geoid and Earth Observation*: 19-24, Springer-Verlag Berlin Heidelberg, ISBN: 978-3-642-10633-0.
6. Tenzer R, Novák P (2010). Effect of the long-wavelength topographical correction on the low-degree Earth's gravity field. In Mertikas SP (ed.) *Gravity, Geoid and Earth Observation*: 355-360, Springer-Verlag Berlin Heidelberg, ISBN: 978-3-642-10633-0.
7. Douša J, Filler F, Šimek J, Kostelecký J, Kostelecký J (jr), Novák P (2011). New implementation of ETRS89 in the Czech Republic: Campaign EUREF-Czech-2009. *Geodetický a kartografický obzor* 55(99): 25-35.

Detection of hidden impact structures on the Earth surface

(responsible person: J. Kloko•ník)

EGM2008 (Earth Gravity Model 2008)

presented in April 2008

creator: **NGA** (National Geospatial Intelligence Agency), USA
Combined model to *l,m* = 2160, 2160 ~ 5' x 5'

Satellite data:

GRACE – model ITG-GRACE03S (*l,m* = 180, 180)

Surface data:

gravity anomalies $\Delta g(\Delta C_{lm}, \Delta S_{lm})$ resolution 5' *x 5', determined from surface, airborne and naval measurements of g* (17.6 *%)*
$\Delta C_{lm}, \Delta S_{lm}$ determined from satellite altimetry (63.2 *%*)
$\Delta C_{lm}, \Delta S_{lm}$ determined from polar mission (Arctis) (3 *%)*
$\Delta C_{lm}, \Delta S_{lm}$ determined from GRACE mission (Antarctis) (16.2 *%*)

EGM08 – data sources

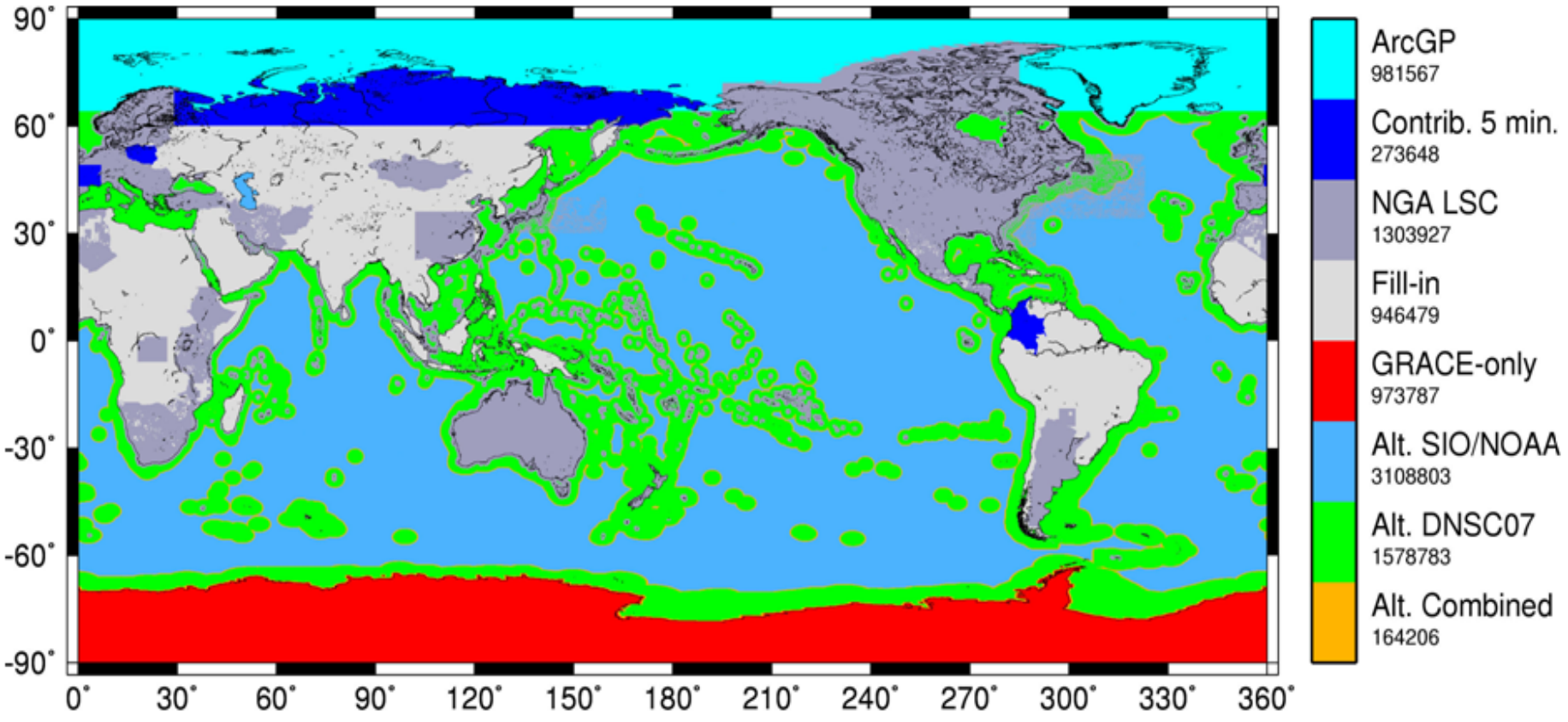

EGM08: commission error at selected locations

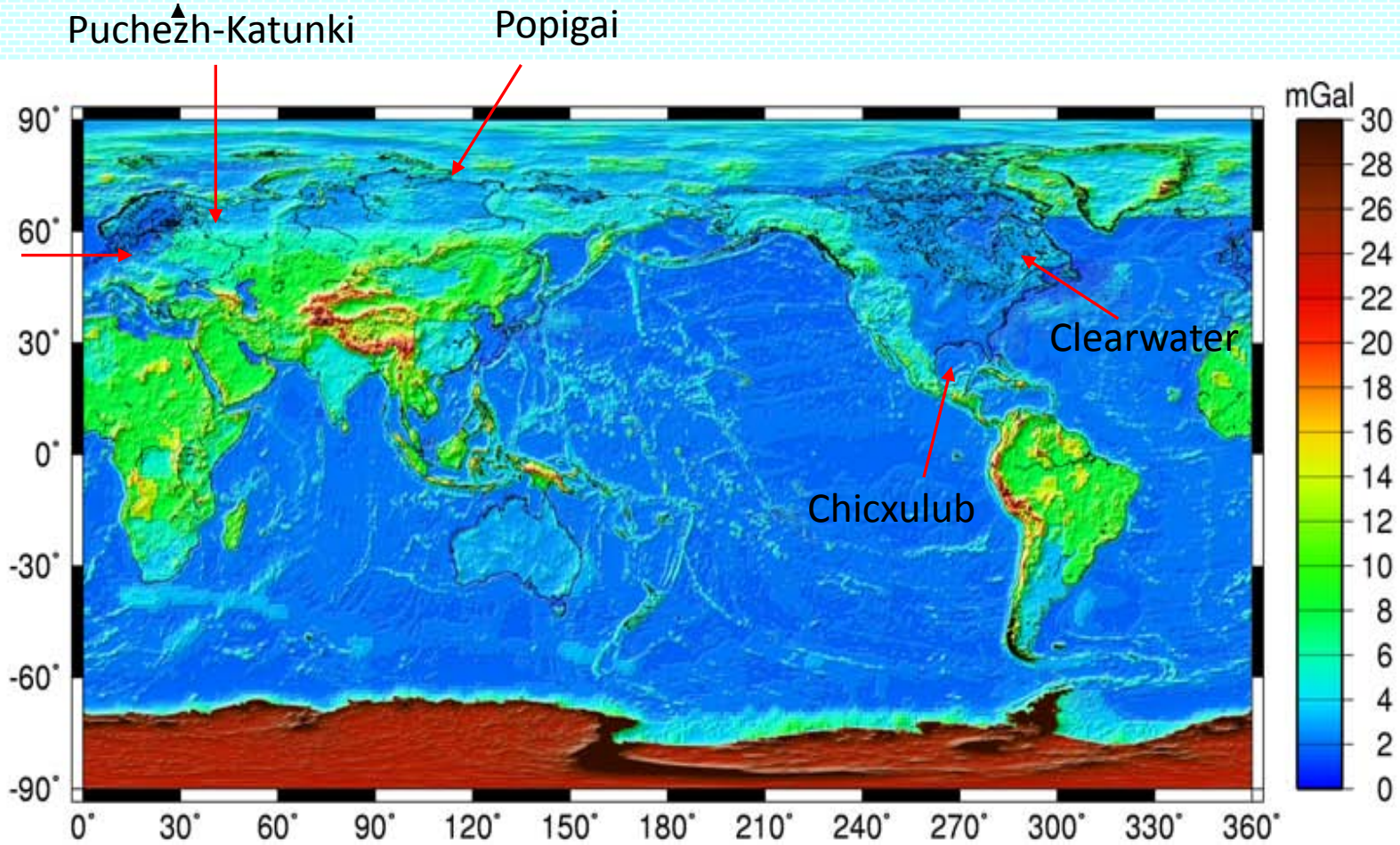

Methodology

- For each locality the gravity anomaly Δg and second radial derivative T_{rr} were computed
- Units: 1 mGal = 10^{-5} m.s^{-2}, 1 mE = 10^{-12} s^{-2}

(1 E corresponds to the change of 1 mGal per 10 km)

- Spherical approximation:

$$\Delta g(r,\theta,\lambda) = -\left(\frac{\partial}{\partial r} + \frac{2}{r}\right) T(r,\theta,\lambda) = \frac{GM}{R^2} \sum_{n=2}^{\max} (n-1) \left(\frac{R}{r}\right)^{n+2} T_n(\theta,\lambda)$$

$$T_{rr}(r,\theta,\lambda) = \frac{\partial^2}{\partial r^2} T(r,\theta,\lambda) = \frac{GM}{R^3} \sum_{n=2}^{\max} (n+1)(n+2) \left(\frac{R}{r}\right)^{n+3} T_n(\theta,\lambda)$$

where

$$T_n(\theta,\lambda) = \sum_{m=0}^{n} \left(C_{n,m} \cos m\lambda + S_{n,m} \sin m\lambda\right) P_{n,m}(\cos\theta)$$

CONFIRMED IMPACT CRATERS TESTED

Name	Location	D *[km]*	t *[My]*
Vredefort	South Africa	300	2020
Sudbury	Ontario, Canada	250	1850
Chicxulub	Yucatán, Mexico	170	65
Popigai	Siberia, Russia	100	35.7
Manicouagan	Quebec, Canada	100	214
Beaverhead	Idaho, United States	100	900
Acraman	South Australia, Australia	90	590
Chesapeake Bay	Virginia, United States	90	35.5
Puchezh-Katunki	Nizhny Novgorod, Russia	80	167
Morokweng	Kalahari Desert, South Africa	70	145
Kara	Nenetsia, Russia	65	70
Woodleigh	Western Australia, Australia	60-120	364
Tookoonooka	Queensland, Australia	55	128
Charlevoix	Quebec, Canada	54	342
Siljan	Dalarna, Sweden	52	377
Kara-Kul	Pamir Mountains, Tajikistan	52	5
Montagnais	Nova Scotia, Canada	45	50
Araguainha	Central Brazil	40	244
Mjølnir	Barents Sea, Norway	40	142
Saint Martin	Manitoba, Canada	40	220
Carswell	Saskatchewan, Canada	39	115
Clearwater West	Quebec, Canada	36	290
Manson	Iowa, United States	35	73.8

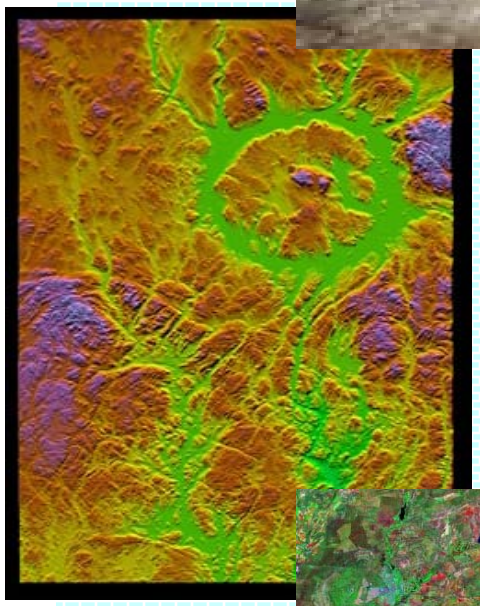

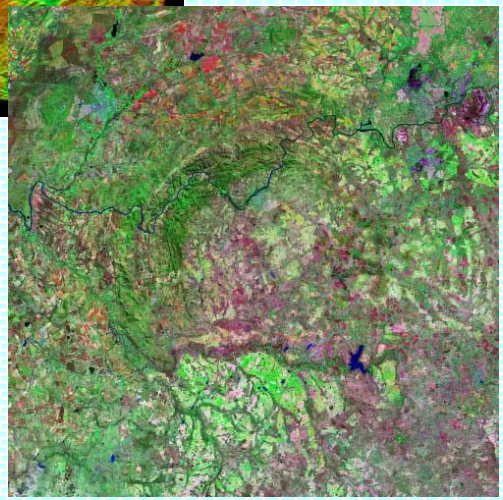

Chicxulub, Yucatan – test area

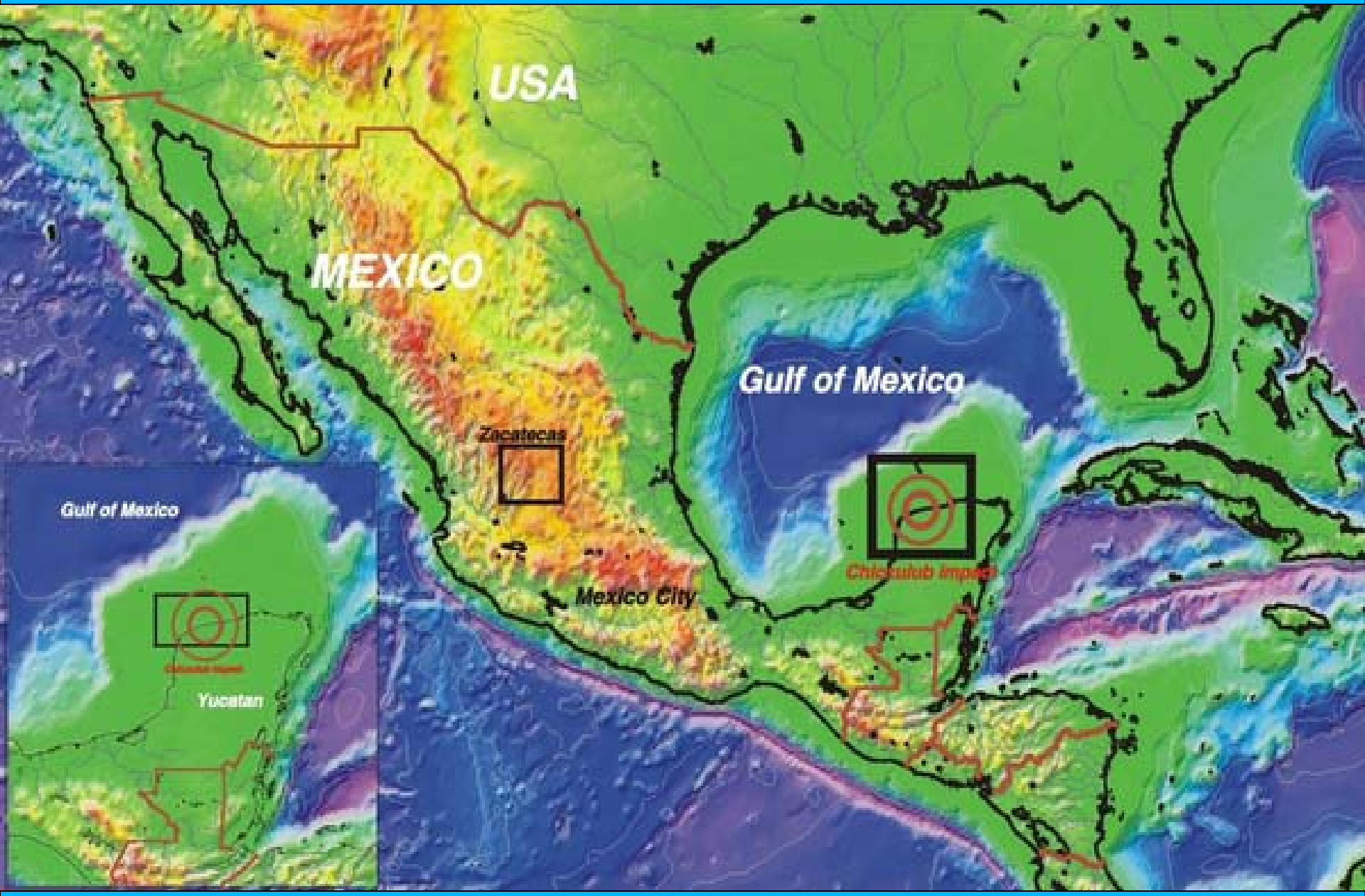

Chicxulub, Yucatan – test area

Each blue dot below represents a cenote such as the one to the left.

Merida

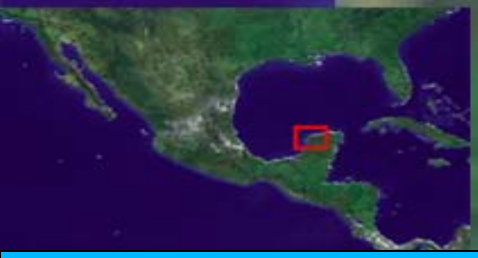

Chicxulub, Yucatan – test area

Δg gravity anomalies from terrestrial measurements

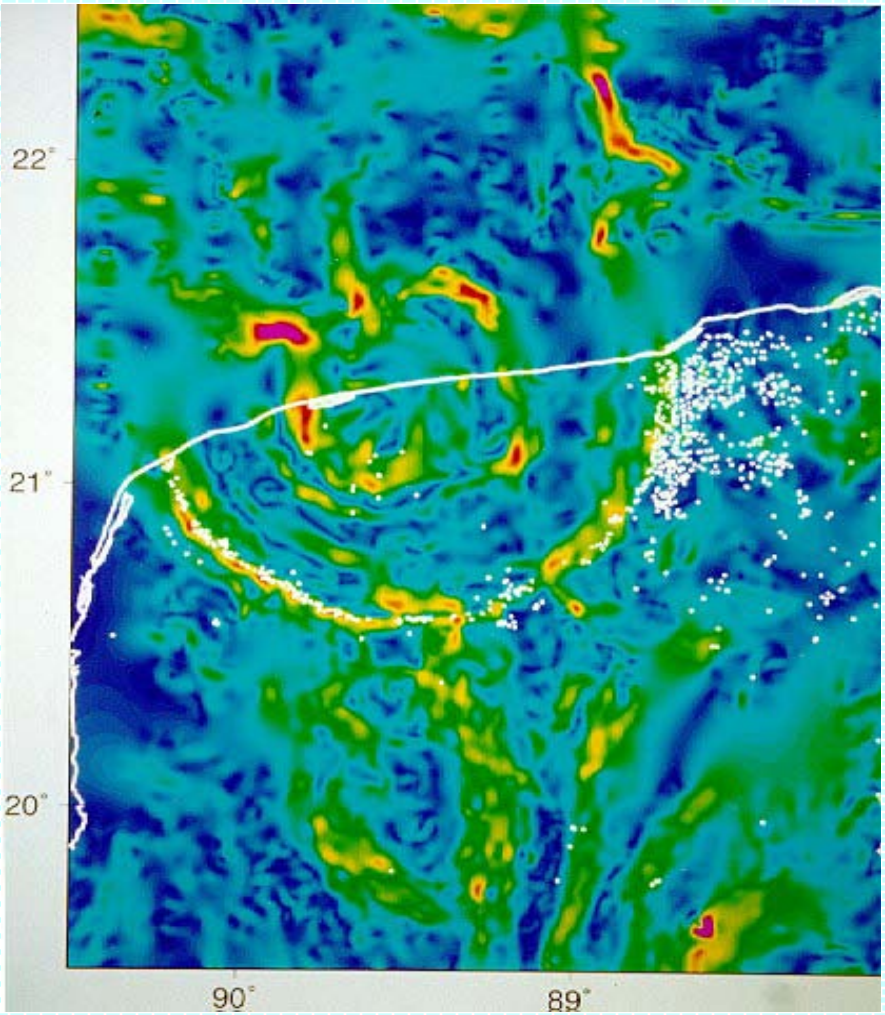

Δg

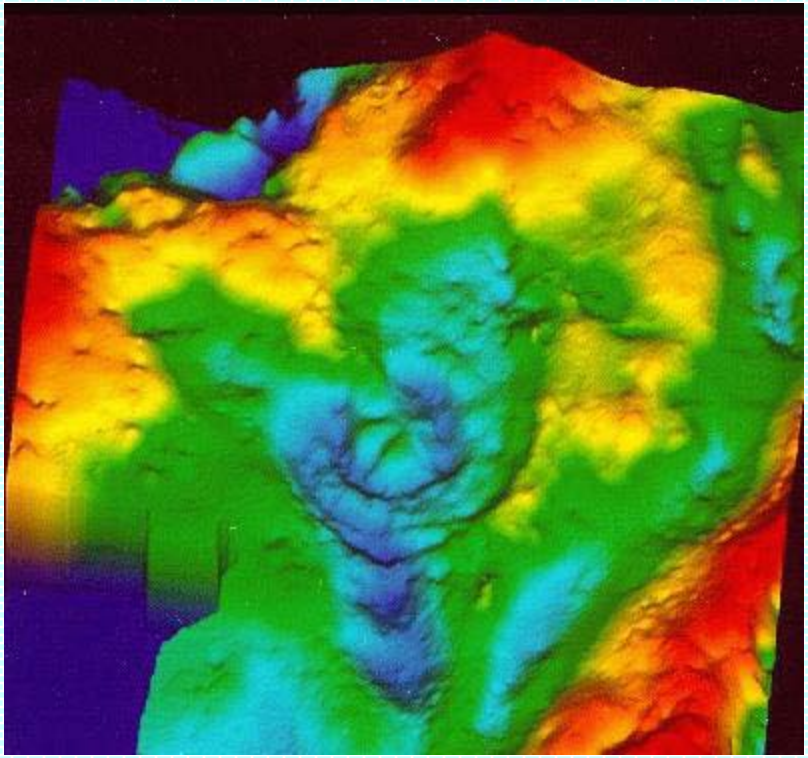

New candidates – Chicxulub II

Δg

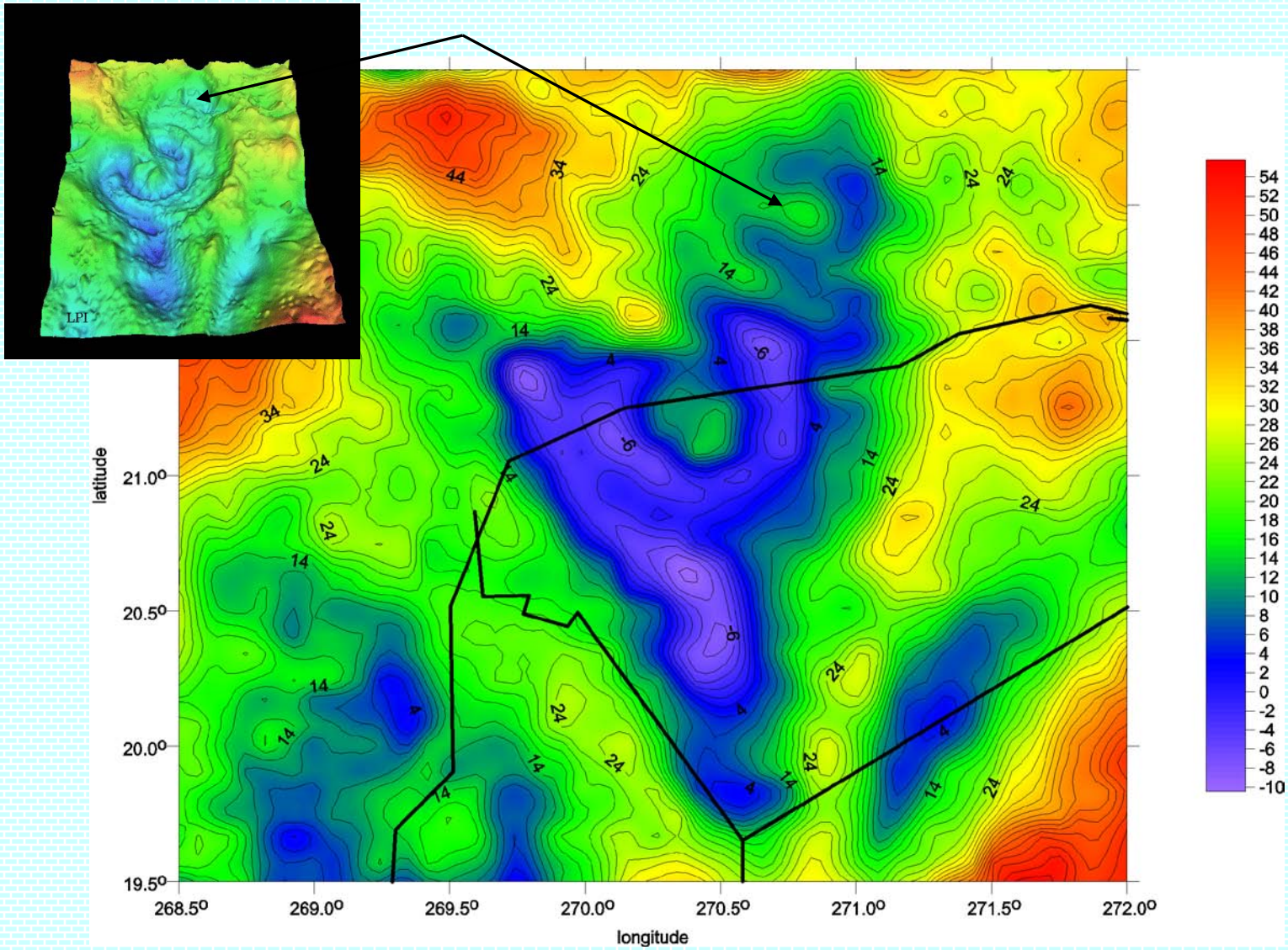

New candidates – Chicxulub II

T_{rr}

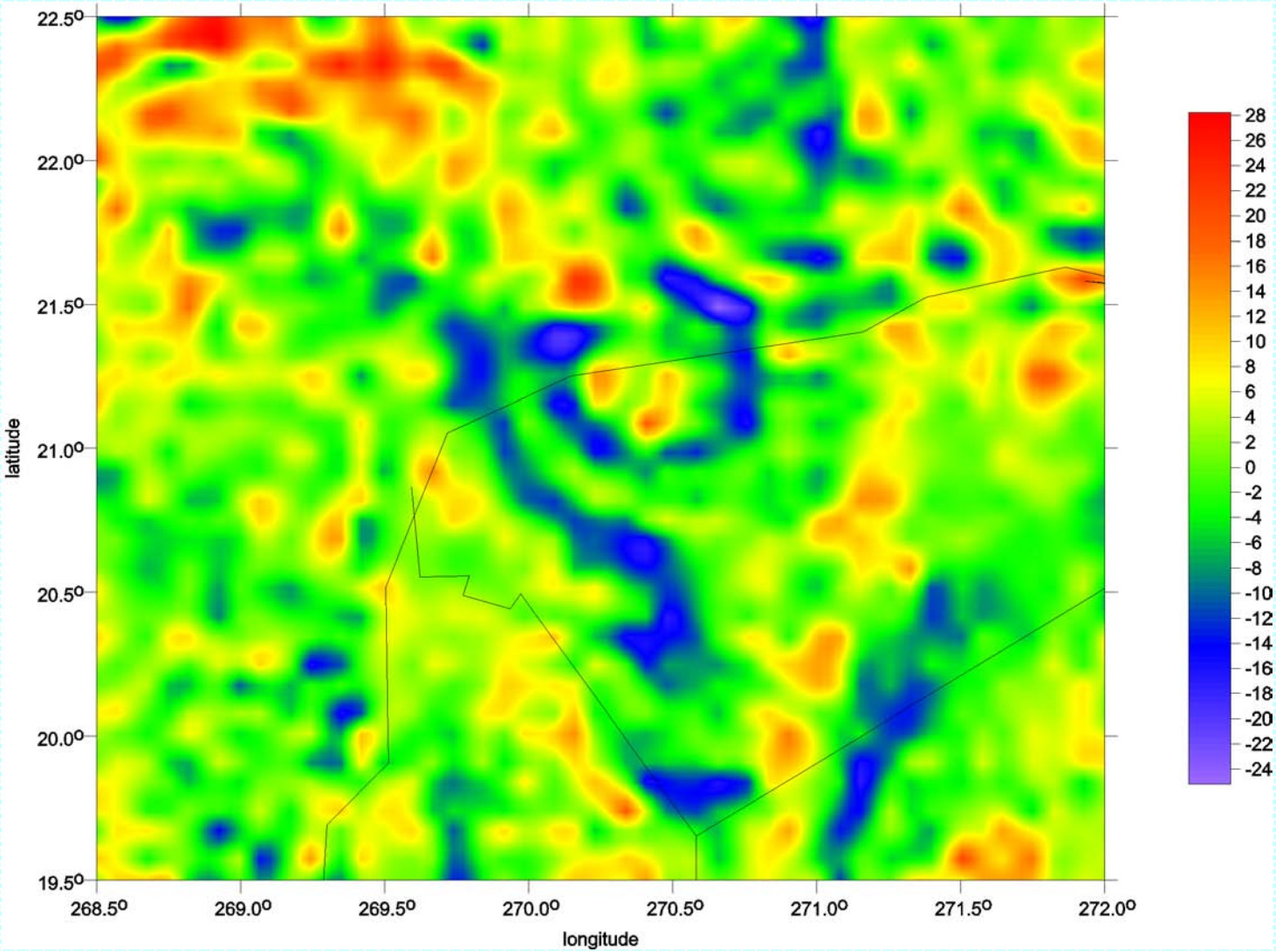

New candidates – Popigai II, etc.

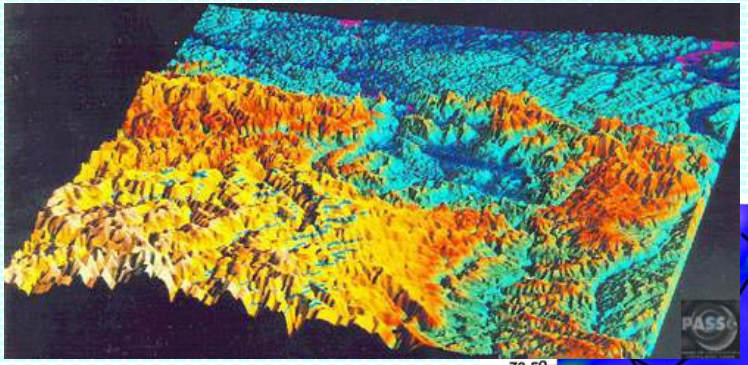

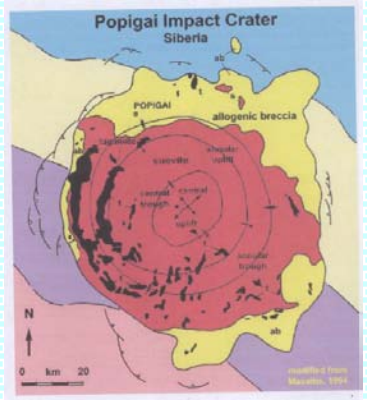

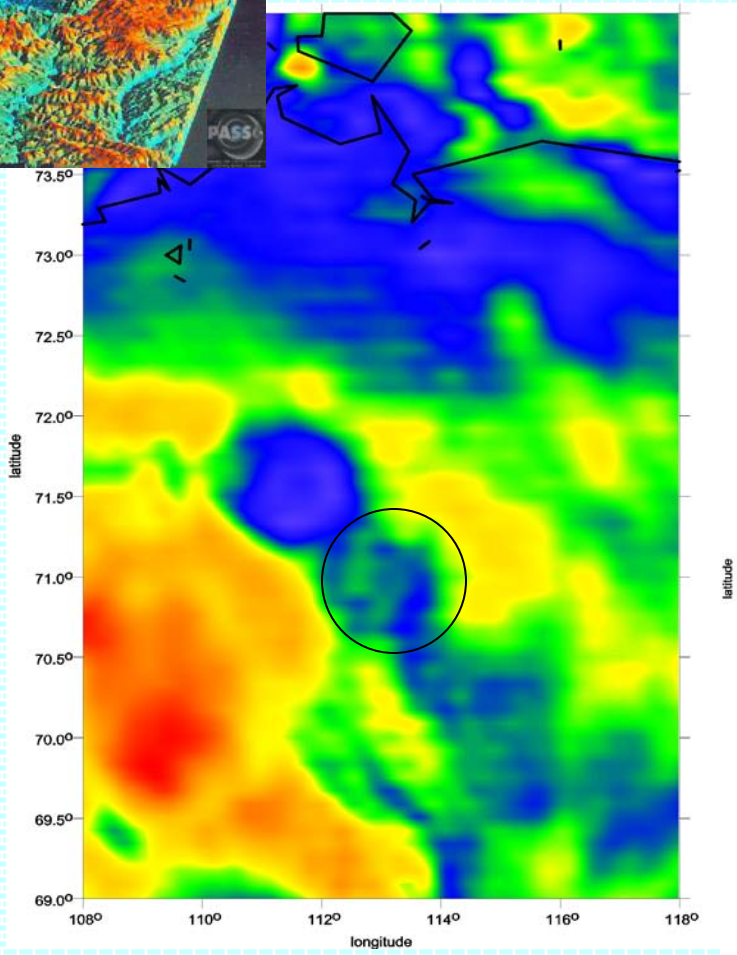

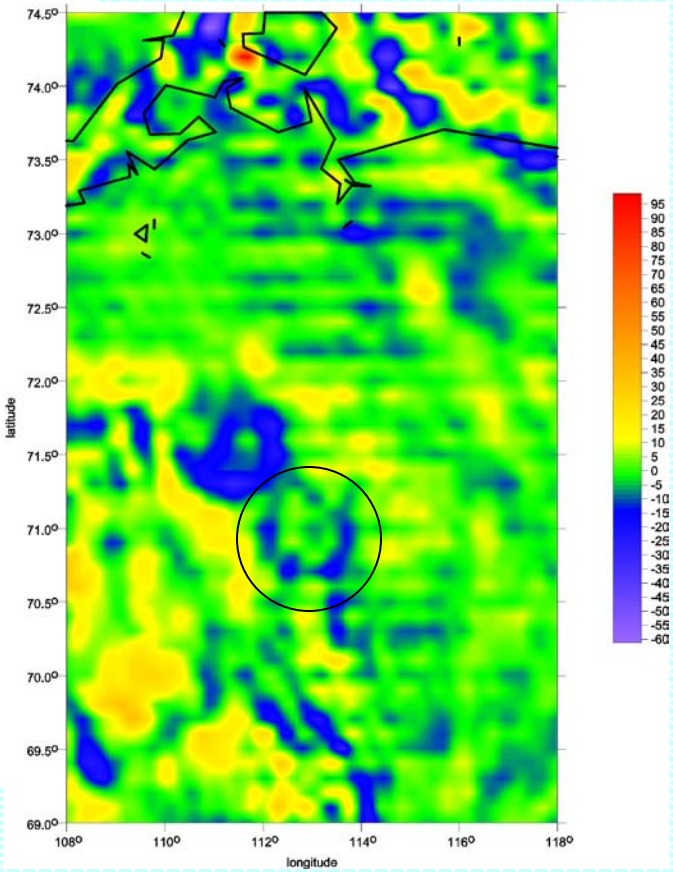

Crater modelling - integration of mass point model with realistic geological data

- **As the craters as well as other structures are often circular, it is convenient to describe the mass distribution using a cylindrical input grid, whose axis is directed upward and axes, to the south and east, respectively, in the plane tangential to the sphere at the origin of the system, the mass element coordinates be azimuth, radius-vector and height above the plane. To retain both the simplicity of the model grid and the fit to the Earth's surface, they can be treated in spherical coordinates, i.e. the radius-vector as a spherical distance and the height as a height above the reference sphere.**
- **The input data is transformed to a local satellite system, with origin at the satellite and axes *x*, *y* to the north and east, respectively, and *z* along the plumb line downward. This allows to integrate the second derivatives using the formulas with the kernels *Kij* for individual derivatives as follows:**
- **Here *G* is (universal) gravitational constant, τ denotes volume of the body, σ its density, and *r*, ε and α are the spherical coordinates of a mass element associated to the *xyz* frame. Indexes *i*, *j* stand for *x*, *y*, *z*.**

$$T_{ij} = G\int_{\tau}\sigma(\tau)K_{ij}\,d\tau$$

$$K_z = r^{-2}\sin\varepsilon \qquad K_{xz} = \frac{3}{2}r^{-3}\sin 2\varepsilon\cos\alpha \qquad K_{yz} = \frac{3}{2}r^{-3}\sin 2\varepsilon\sin\alpha$$

$$K_{xy} = \frac{3}{2}r^{-3}\cos^2\varepsilon\sin 2\alpha \qquad K_{yy} = r^{-3}(3\cos^2\varepsilon\sin^2\alpha - 1) \qquad K_{zz} = r^{-3}(3\sin^2\varepsilon - 1)$$

$$K_{xx} = r^{-3}(3\cos^2\varepsilon\cos^2\alpha - 1)$$

…. - Clearwater, Quebec, Canada – test area

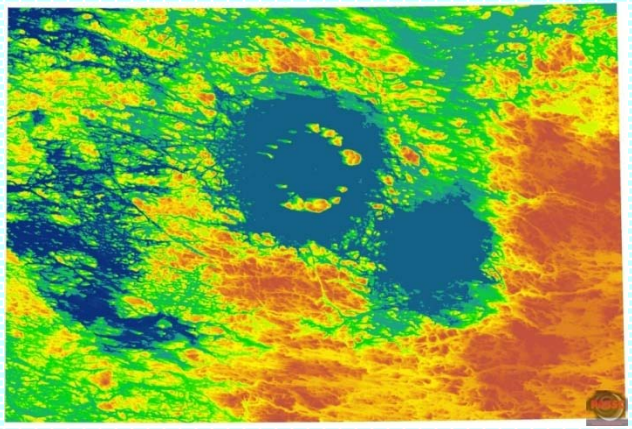

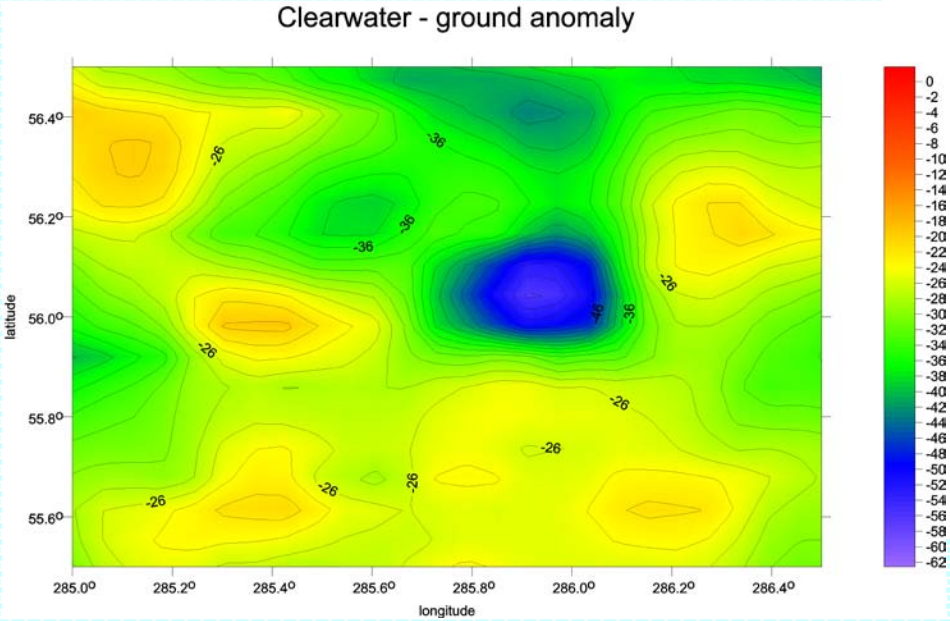

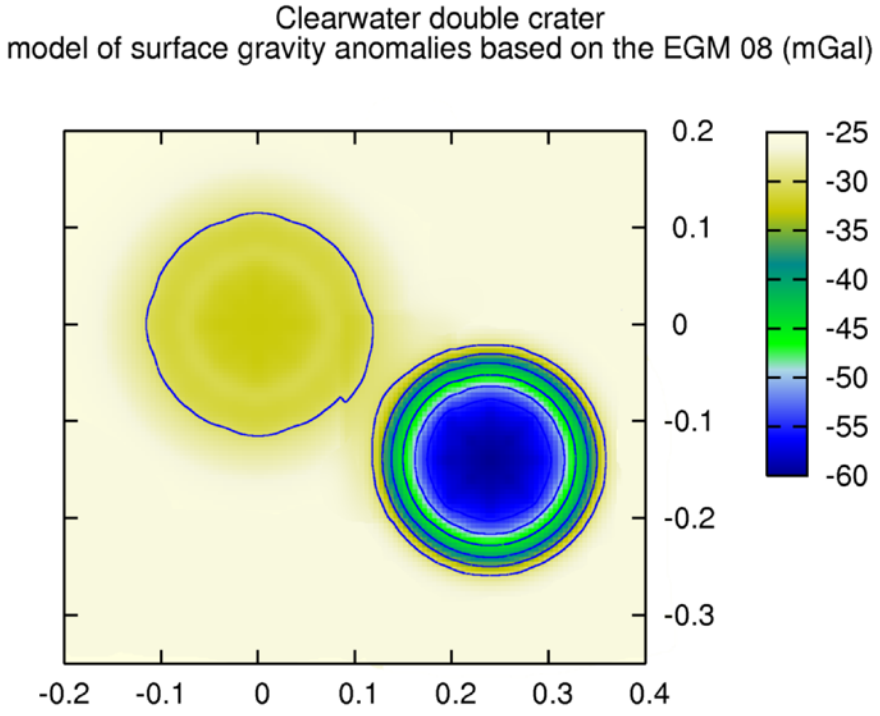

…. Crater modelling – Chicxulub

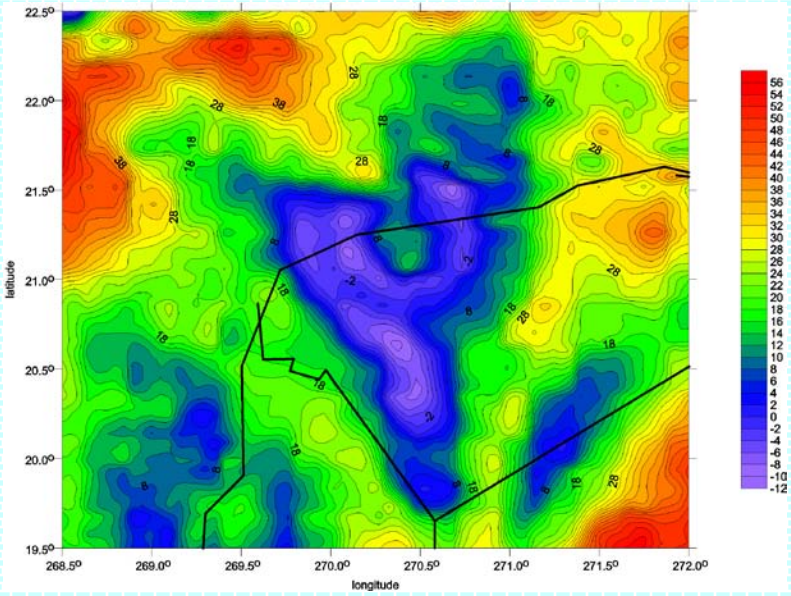

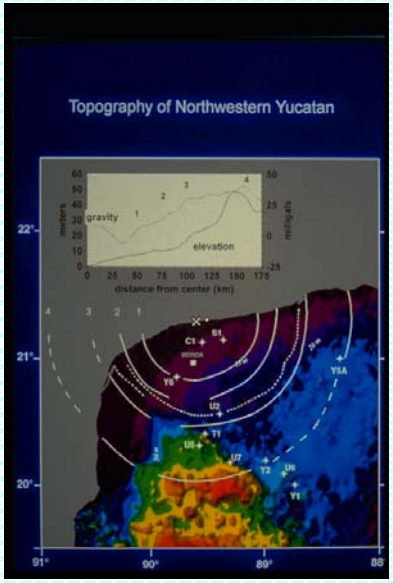

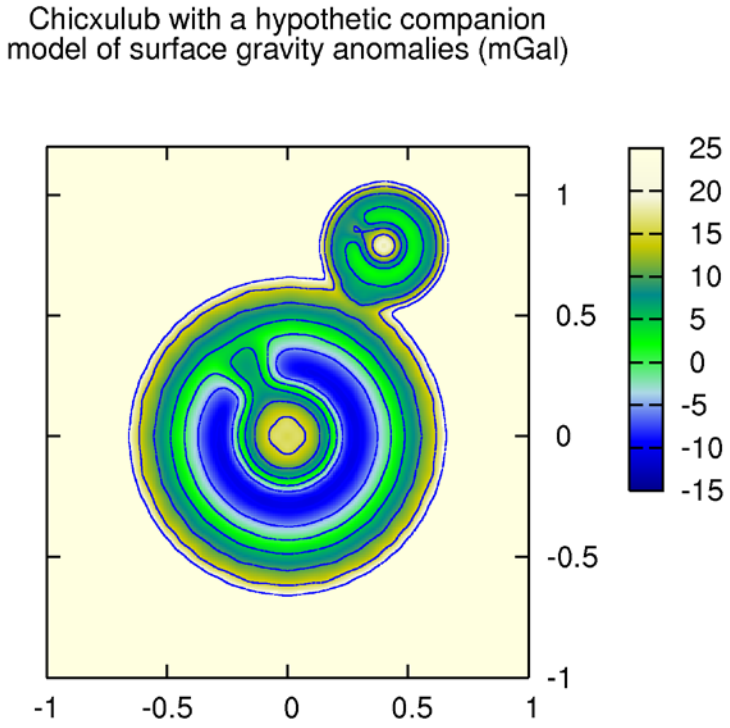

Model:
Main crater without rings, diameter ~ 150 km,
“remove-restore” method
(reduction of gravity anomalies around the main crater by 25 mGal)

…. - Crater modelling - Popigai

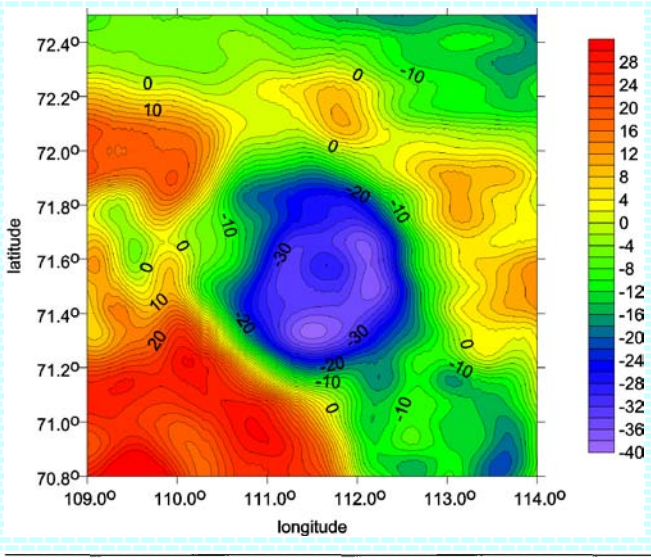

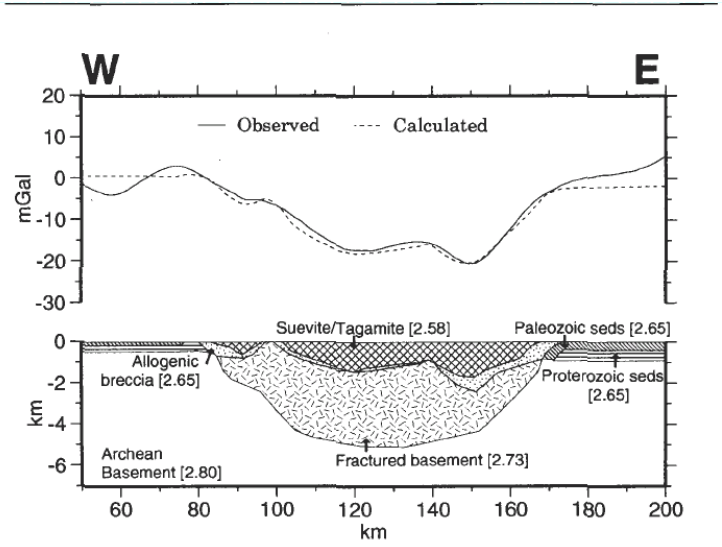

Fig. 8. Final gravity model. Densities are given in gcm^{-3}. See Fig. 1 for profile location.

Popigai with a hypothetic companion
model of surface gravity anomalies (mGal)

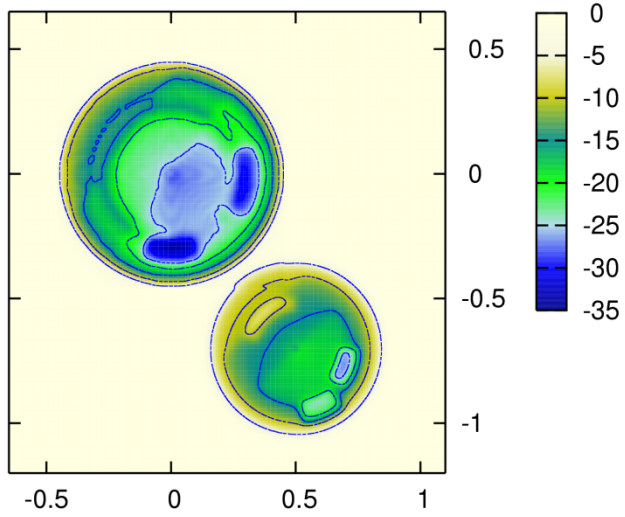

Popigai with a hypothetic companion
model of gravity anomalies at altitude of 1.5 km (mGal)

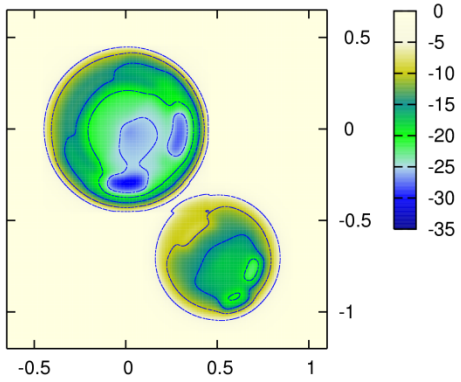

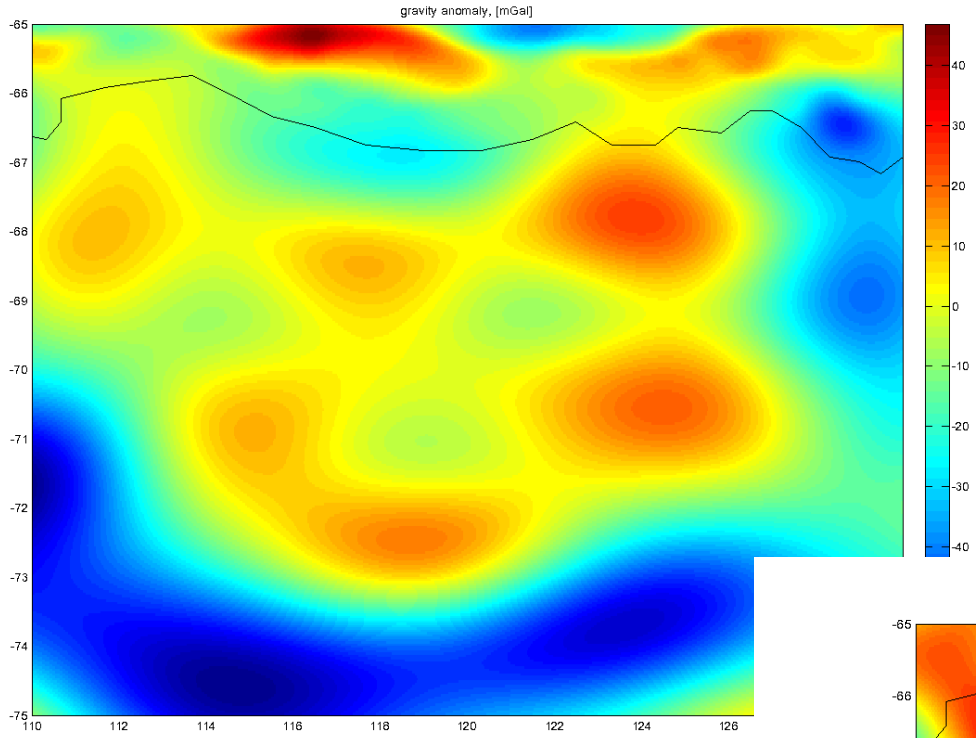

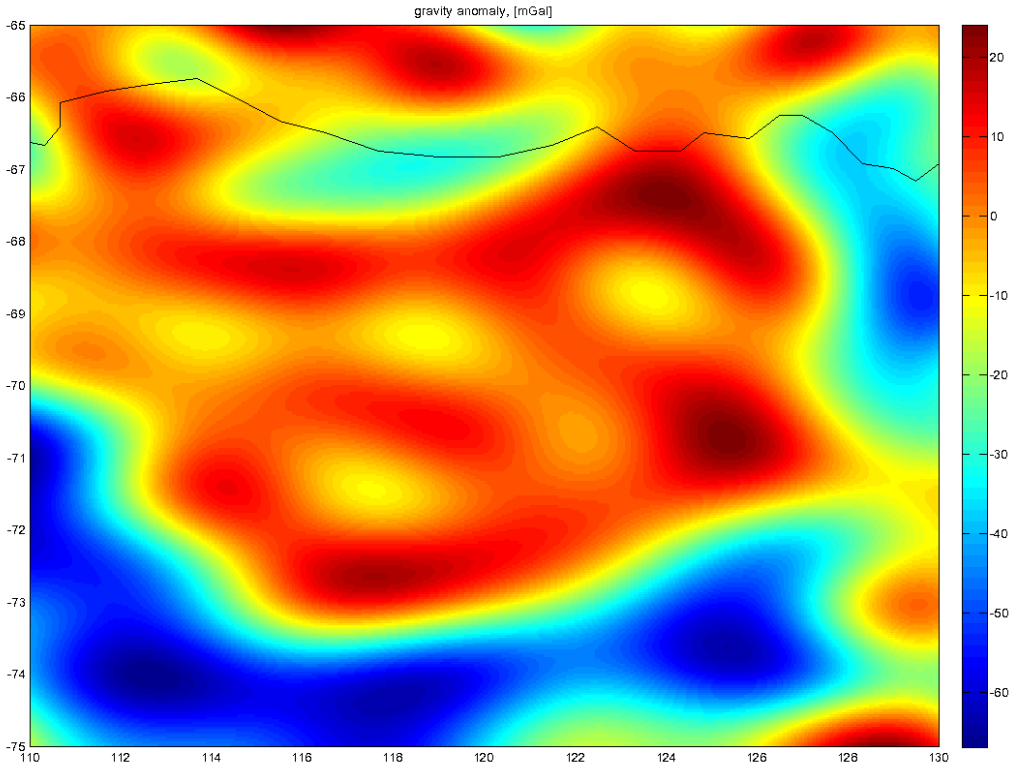

Wilkis Land, Antarctis

CORRELATION GRAVITY VS. MORPHOLOGY
(J. Kloko• ník, J. Kostelecký;
J. Kalvoda, Charles University, Prague)

- Example – Himalaya, Nepal

DISTRIBUTION OF MIN/MAX T_{rr}

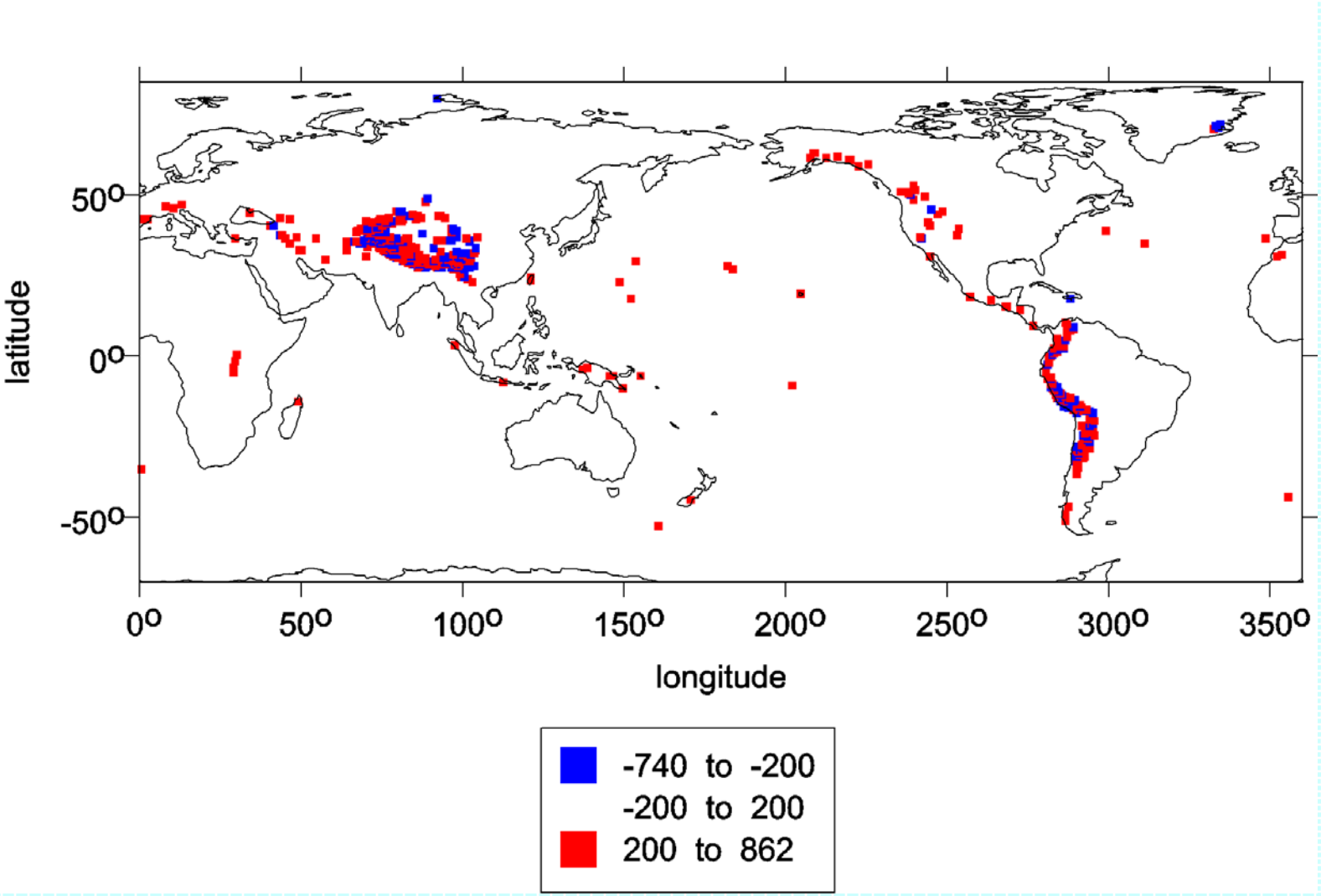

Gravity anomalies • g, Himalaya

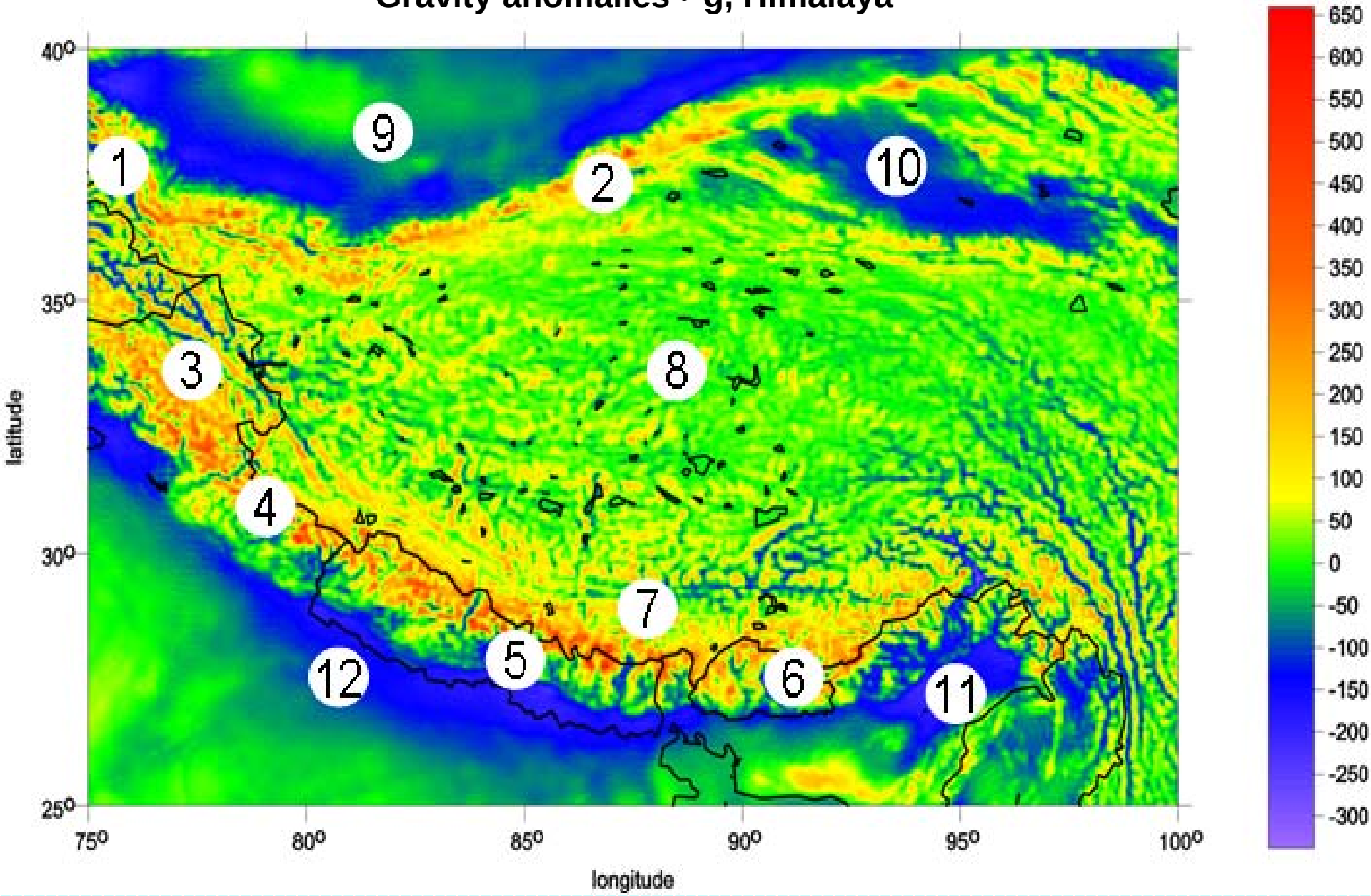

Second radial derivatives T_{rr} , Himalaya

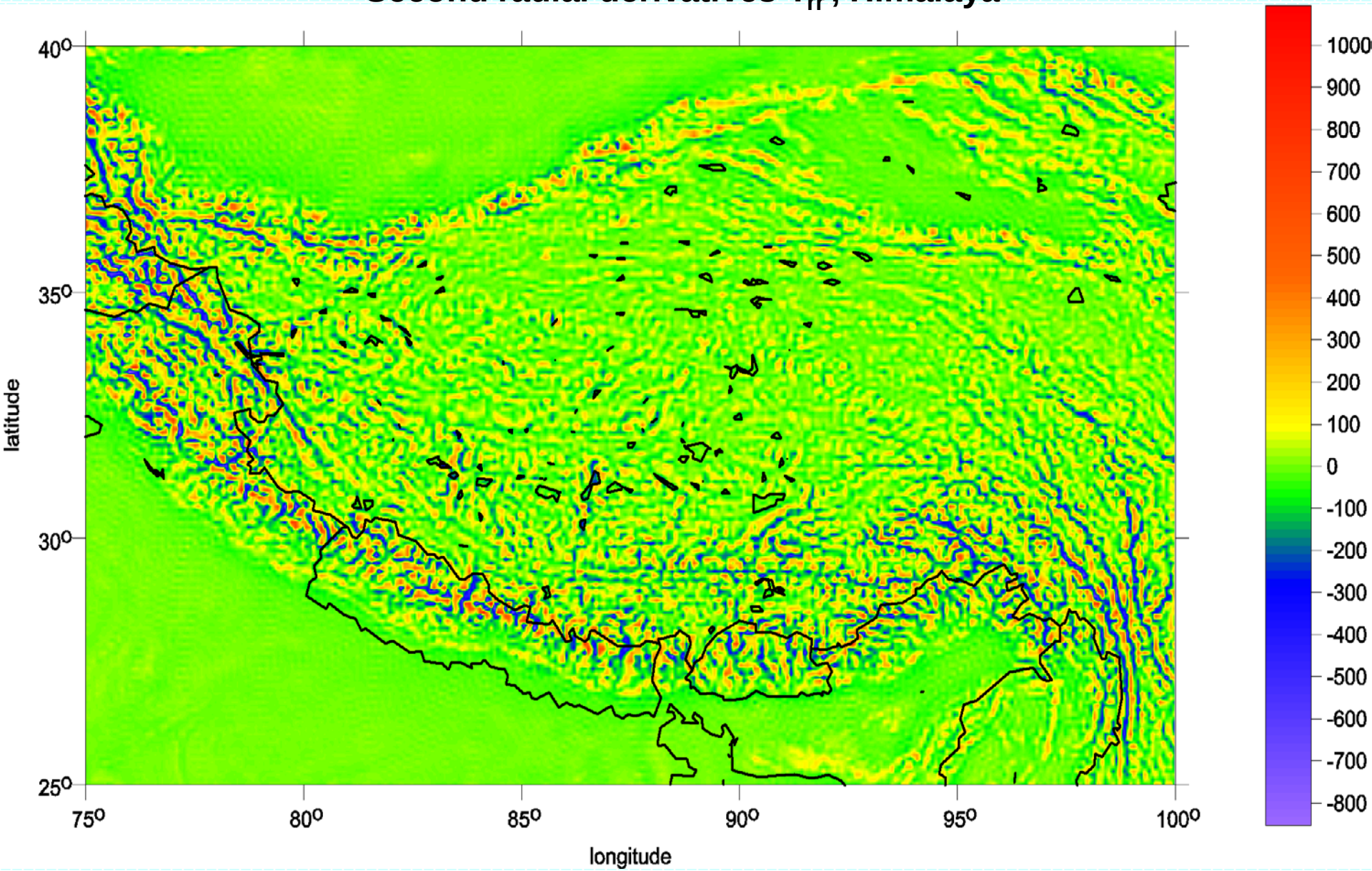

• g

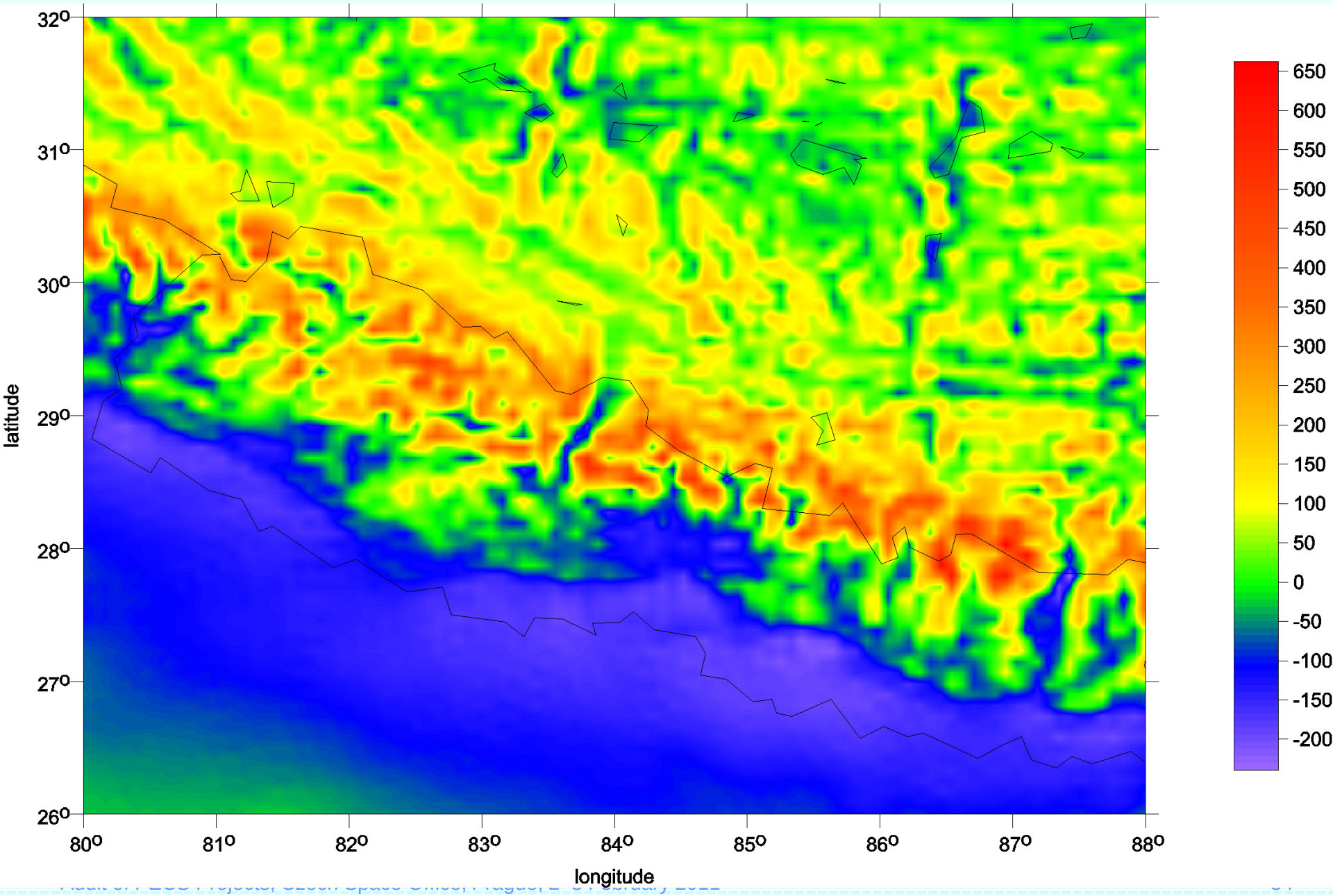
32°
31°
30°
29°
28°
27°
26°
latitude
80°
81°
82°
83°
84°
85°
86°
87°
88°
longitude
650
600
550
500
450
400
350
300
250
200
150
100
50
0
-50
-100
-150
-200

T_{rr}

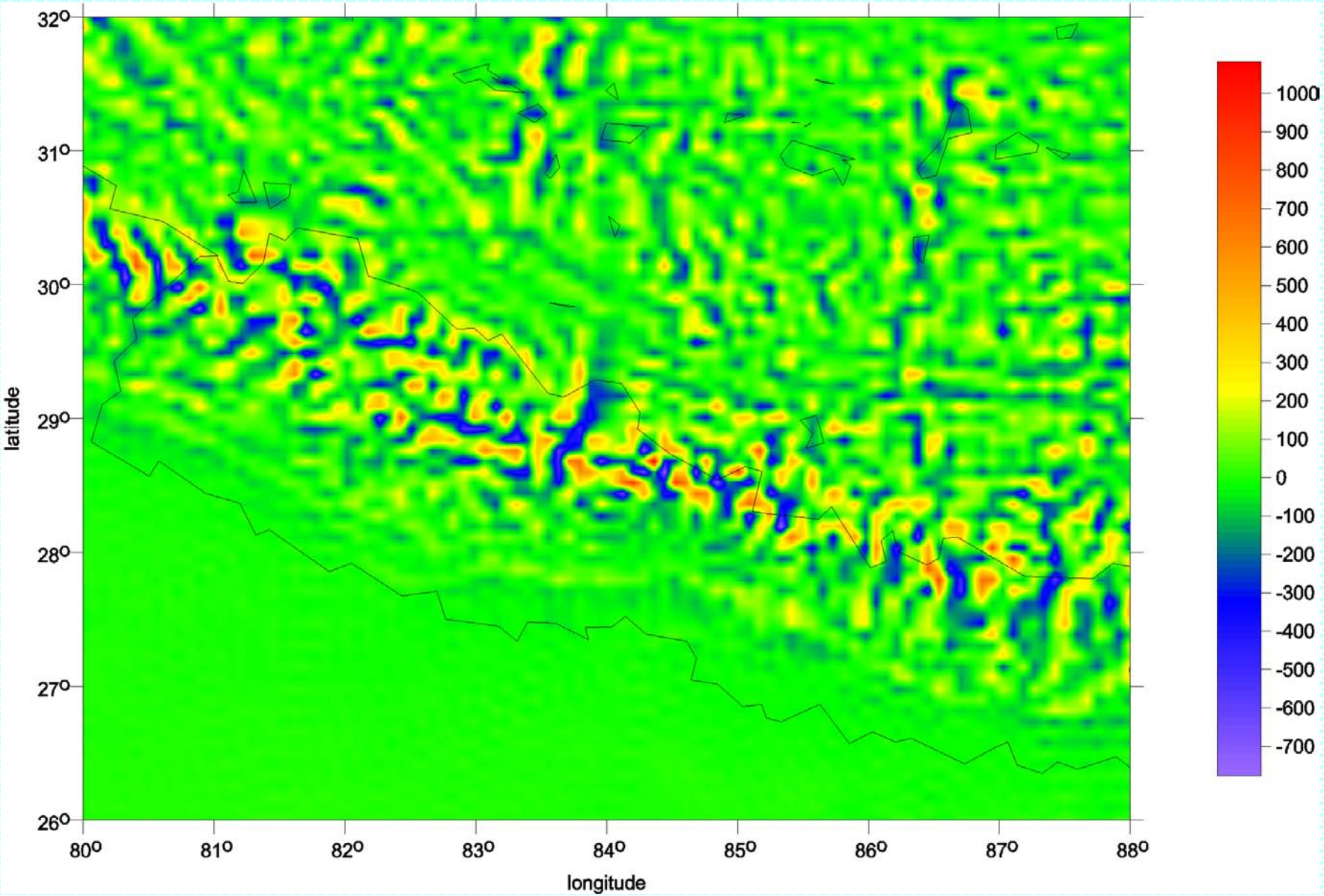
32°
31°
30°
29°
28°
27°
26°
latitude
80°
81°
82°
83°
84°
85°
86°
87°
88°
longitude
1000
900
800
700
600
500
400
300
200
100
0
-100
-200
-300
-400
-500
-600
-700

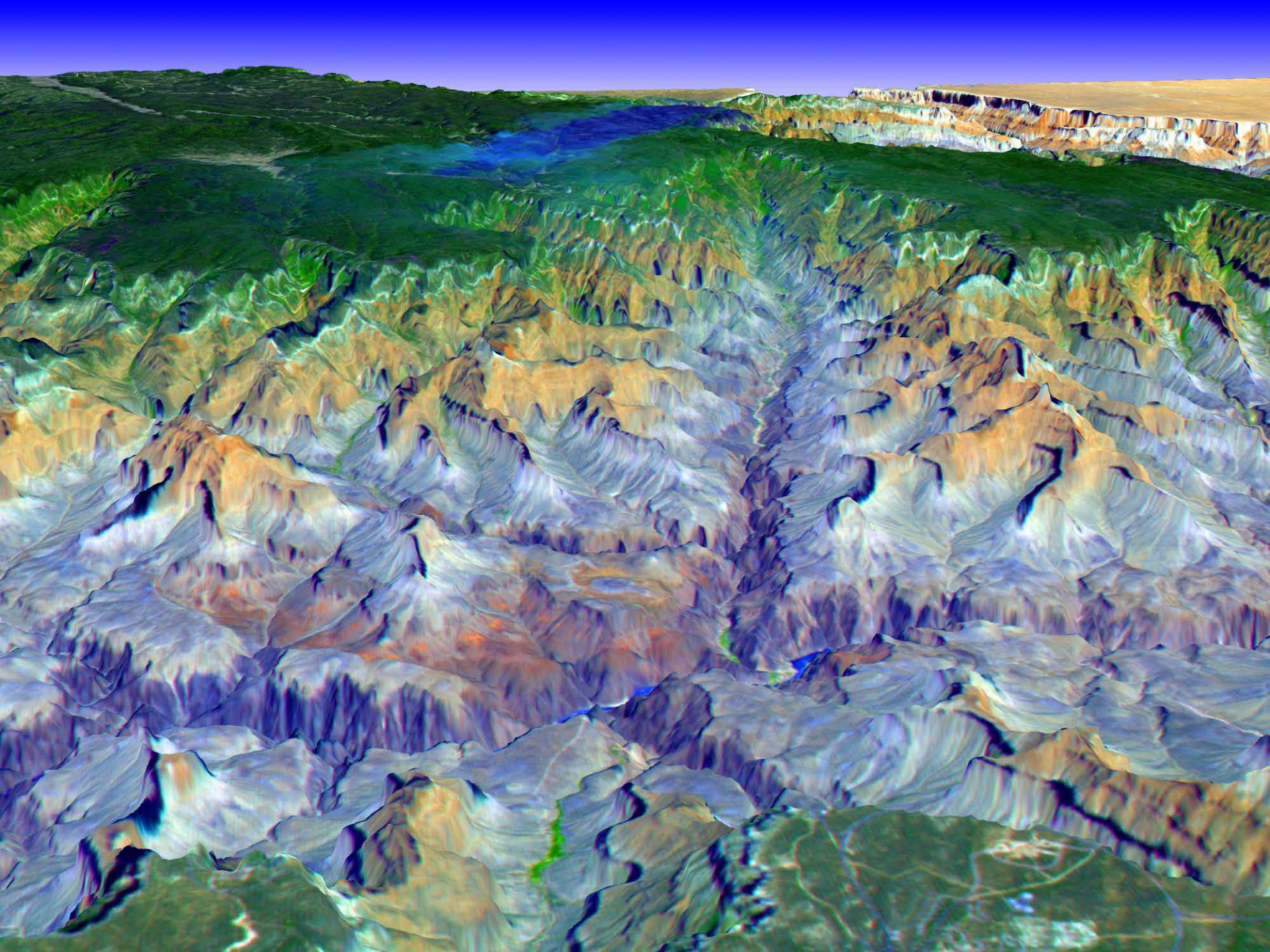

CORRELATIONS “GRAVITY VS. MORPHOLOGY”

- Strong coincidences between large-scale morphogenetic styles of the Nepal Himalaya and the extension of regions with very high positive values of the radial second derivative of the disturbing gravitational potential T_{rr} and the most likely in combination with conspicuous areas of high negative values of T_{rr} in their close neighbourhood, have been identified. These variable values of T_{rr} display significant gravitational signatures of extensive differences and changes in mass density and/or rock massif and regolith distributions which occurred during very dynamic landform evolution of the Nepal Himalaya in the late Cenozoic.

CONCLUSIONS

- **Founded correlations:**
  - **high horizontal gradient of T_{zz} … dynamical changes of morphology**
  - **low horizontal gradient of T_{zz} … morphologically “quiet” landscape**

- ***Published or submitted contributions:***

1. Kloko• ník J., Novák P., Kostelecký J., Wagner C.A., Detecting impact craters using the EGM 08, Acta Geodyn. Geomater. 2010, 7, #1 (157), 71-97.
2. Kloko• ník J., Kostelecký J., Pešek I., Novák P., Wagner C.A., Sebera J., Candidates for multiple impact craters?: Popigai and Chicxulub as seen by the global high resolution gravitational field model EGM08, Solid Earth EGU 2010, 1, 71-83, DOI: 10.5194/se-1-71-2010.
   See also: Is Chicxulub a double impact crater? Pres. at 6th EGU A. von Humboldt Interntl. Conf. on Climate Change, Natural Hazards, and Societies, Mérida, México, section: The Cretaceous/Tertiary Boundary
3. Pešek I., Wagner C.A., Kloko• ník J., Kostelecký J., Sebera J., EGM 08 searches for hidden impact craters, with support from point mass modelling, Pres. at EGU GA Vienna 2010, Geophys. Res. Abstracts 12, EGU2010-2121, 2010.
4. Kostelecký J., Kloko• ník J., Pešek I., Kalvoda J.: Possible applications of detailed Earth´s gravity field model. Presented on the „11th Czech-Polish workshop „On recent geodynamics of the Sudeten and adjacent areas“, Castle T•eš•, 4 – 6 November 2010. [5] Kalvoda J., Kloko• ník J, Kostelecký J. (in print): Regional correlation of the Earth Gravitational Model 2008 with morphogenetic patterns of the Nepal Himalaya. – Acta Universitatis Carolinae, Geographica, XLV, 2, 53 – 78, Prague. (2010) (SCOPUS)
5. Kostelecký J., Kloko• ník J., Pešek I., Kalvoda J.: N• které možné aplikace model• gravita• ního pole Zem• . P•edneseno na seminá•i s mezinárodní ú• astí „Družicové technologie a sú• asná geodézia“, Stavebná fakulta STU Bratislava, 8.12.2010.
6. Kalvoda J., Kloko• ník J., Kostelecký J. (in print): Comparison of morphogenetic features of the Nepal Himalaya with the Earth Gravitational Model 2008. Sborník konferen• ních p•ísp• vk• XXII. Sjezdu • eské geografické spole• nosti, Ostrava 2010, 9 p., 8 figs. (ISI / Proceedings – Conference Proceedings Citation Index, Thomson / Reuthers).

EVENTS

- **EGU 6th Alex. von Humboldt conf., Mérida, México, 17 – 19 March 2010**
- **Carolinum Prague, Czech Republic, 30 April 2010**
  J. Kloko• ník named University Professor of the Czech Technical Univ.
- **EGU General Assembly, Vienna, Austria, 2 – 7 May 2010**
- **GOCE Summer school, Herrsching, Germany, 31 May – 4 June 2010**
- **ESA Workshop in Bergen, Norway, 28 June – 2 July 2010**
- **WEGENER 2010, Istanbul, Turkey, 14 – 17 Sept 2010**
- **ESA GNSS-R 2000, workshop on GNSS reflectometry, Barcelona, Spain, 21 – 22 October 2010**
- **AGU General Assembly, Session "The GOCE Gravity Field Mission – Status and Results from the first Year of Science Operation",**
  San Francisco, USA, 13 – 17 Dec 2010

Prezident
republiky

Vážený pan

doc. Ing. Jaroslav K l o k o č n í k , DrSc.
nar. 2. srpna 1948

Na návrh Vědecké rady Českého vysokého učení technického v Praze, podle § 73 zákona č. 111/1998 Sb., o vysokých školách a o změně a doplnění dalších zákonů (zákon o vysokých školách),

Vás jmenuji,
s účinností od 1. května 2010,

p r o f e s o r e m
pro obor geodézie a kartografie.

Prezident republiky

Předseda vlády

V Praze dne 2. dubna 2010

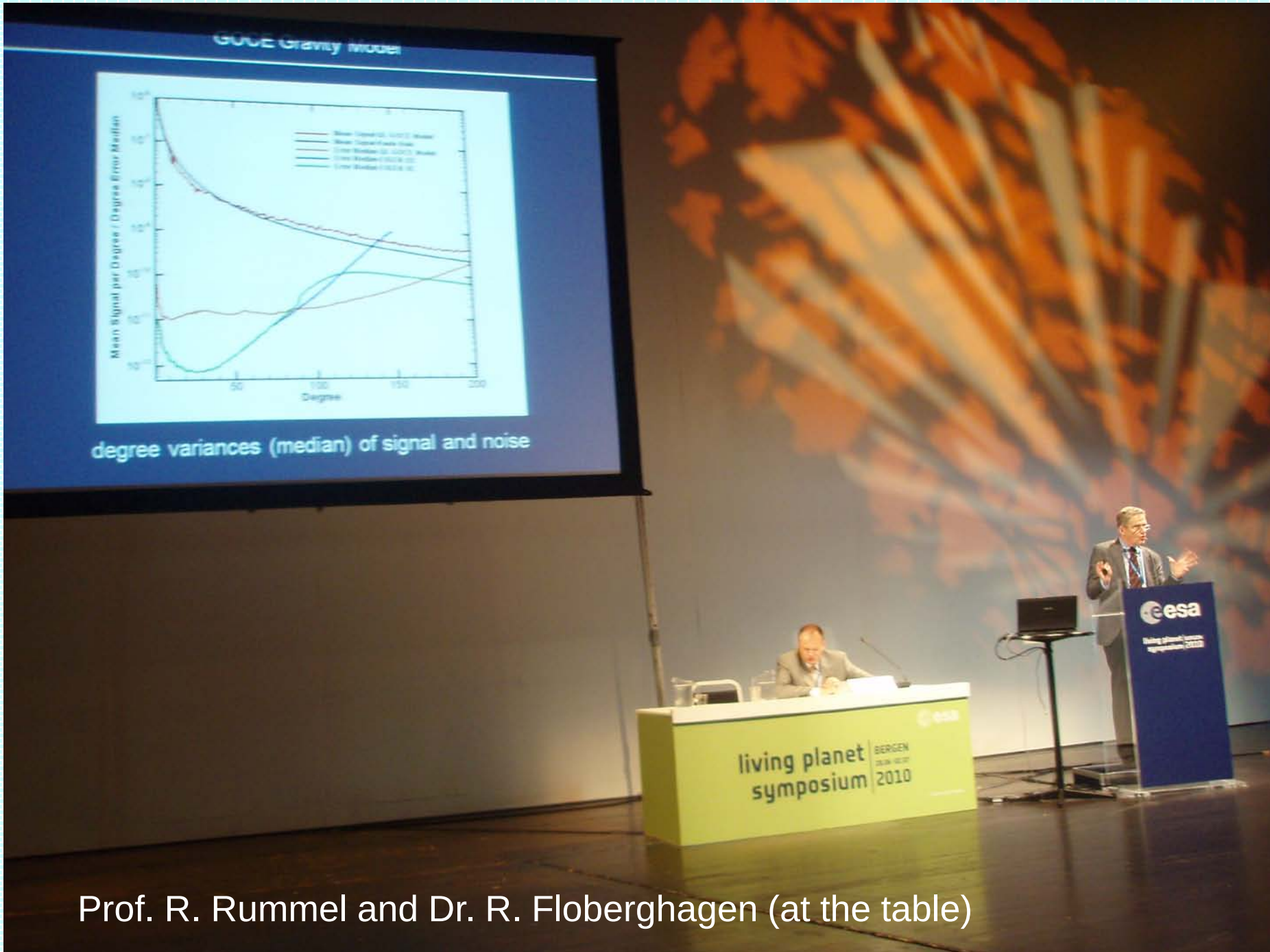

Prof. R. Rummel and Dr. R. Floberghagen (at the table)

Dr. A. Bezd• k

Ing. J. Sebera

Financial Plan for 2010 and its fulfilment

ITEM		AMOUNT (€)	
		planned	realized
Salaries incl. all insurances		46 400	**28 800**
Travel (incl. tickets, per diem, accommodation, fees, etc.)		9 000	18 500
Small equipment - smaller then 5000 Euro per piece		2 000	1 200
Large equipment		0	0
Miscellaneous	data GOCE, system eng. consultations	1 000	0
	publications of colour pages	500	0
	consumables	300	300
	services	500	**11 100**
Overheads		500	300
Total		**60 200**	**60 200**

Small changes in the Financial Plan:

- Sum for Services • falls in fact under Salaries (salary of Prof. J. Kostelecký and Ing. I. Pešek, CTU)
- Somewhat higher travel expenses – due to a busy year in the GOCE related international meetings

In total, the **sum planned** and the sum **actually paid** in 2010 are the **same**

Thank you for your attention